Title

Bypassing the Requirement for an Essential MYST Acetyltransferase

Journal

Genetics, 197(3)

ISSN

0016-6731

Authors

Torres-Machorro, Ana Lilia

Pillus, Lorraine

Publication Date

2014-07-01

DOI

10.1534/genetics.114.165894

Peer reviewed

Bypassing the Requirement for an Essential MYST Acetyltransferase

Ana Lilia Torres-Machorro and Lorraine Pillus[1]
Section of Molecular Biology, Division of Biological Sciences, University of California, San Diego, UC San Diego Moores Cancer Center, La Jolla, California 92093-0347

ABSTRACT Histone acetylation is a key regulatory feature for chromatin that is established by opposing enzymatic activities of lysine acetyltransferases (KATs/HATs) and deacetylases (KDACs/HDACs). Esa1, like its human homolog Tip60, is an essential MYST family enzyme that acetylates histones H4 and H2A and other nonhistone substrates. Here we report that the essential requirement for *ESA1* in *Saccharomyces cerevisiae* can be bypassed upon loss of Sds3, a noncatalytic subunit of the Rpd3L deacetylase complex. By studying the *esa1*Δ *sds3*Δ strain, we conclude that the essential function of Esa1 is in promoting the cellular balance of acetylation. We demonstrate this by fine-tuning acetylation through modulation of HDACs and the histone tails themselves. Functional interactions between Esa1 and HDACs of class I, class II, and the Sirtuin family define specific roles of these opposing activities in cellular viability, fitness, and response to stress. The fact that both increased and decreased expression of the *ESA1* homolog *TIP60* has cancer associations in humans underscores just how important the balance of its activity is likely to be for human well-being.

THE genetic information of DNA is packed into chromatin, which is predominantly composed of the H3, H4, H2A, and H2B core histone proteins that together with DNA form nucleosomes, the basic subunits of the genome (Kornberg and Lorch 1999). Chromatin structure regulates many cellular processes including gene expression, DNA replication, DNA damage repair, and recombination (Felsenfeld and Groudine 2003). Nucleosomes themselves are tightly regulated by mobilization and positioning that are mediated by ATP-dependent chromatin-remodeling machines (Rando and Winston 2012) and by multiple types of histone post-translational modifications that include acetylation and many other marks (Campos and Reinberg 2009).

Nucleosome acetylation is a highly dynamic modification that is promoted by HATs and removed by HDACs. HATs are classified by sequence into different families (Allis *et al.* 2007). *ESA1/KAT5* belongs to the widely conserved MYST HAT family, named for its founding members (***M**OZ-**Y**BF2/**S**AS3-**S**AS2-**T**IP60*) (Lafon *et al.* 2007). Esa1 is an essential HAT in yeast (Smith *et al.* 1998; Clarke *et al.* 1999) and the catalytic subunit of two distinct multi-protein complexes: NuA4 and Piccolo (Boudreault *et al.* 2003). Notably, the human homolog of Esa1 is Tip60, which is also essential in vertebrates and has been linked to multiple human diseases (Squatrito *et al.* 2006; Avvakumov and Côté 2007; Lafon *et al.* 2007), thus increasing the relevance of gaining a deeper understanding of essential HAT functions.

Esa1 primarily acetylates H4 and H2A *in vivo* (Clarke *et al.* 1999; Lin *et al.* 2008) and regulates the expression of active protein-encoding genes (Reid *et al.* 2000; Lin *et al.* 2008). It plays a crucial role in cell cycle progression and ribosomal DNA (rDNA) silencing (Clarke *et al.* 1999, 2006) and is recruited to DNA double-strand breaks (DSBs) to promote damage repair by acetylating H4, an important step in the repair pathway (Bird *et al.* 2002; Tamburini and Tyler 2005). Esa1 also regulates replicative life span and autophagy by acetylating the nonhistone targets Sip2 (regulatory subunit of the Snf1 complex, the yeast AMP-activated protein kinase, or AMPK) (Lu *et al.* 2011) and Atg3 (autophagy signaling component) (Yi *et al.* 2012). Due to Esa1's essential nature, to date, hypomorphic and conditional *ESA1* alleles have been critical tools in defining its functions (Clarke *et al.* 1999; Decker *et al.* 2008; Lin *et al.* 2008; Mitchell *et al.* 2008, 2011). The *esa1-414* allele is a frameshift mutation in codon 414 that leads to a C-terminal

doi: 10.1534/genetics.114.165894
Manuscript received February 21, 2014; accepted for publication May 7, 2014; published Early Online May 14, 2014.
Supporting information is available online at http://www.genetics.org/lookup/suppl/doi:10.1534/genetics.114.165894/-/DC1.
[1]Corresponding author: University of California, San Diego, 9500 Gilman Dr., La Jolla, CA 92093-0347. E-mail: lpillus@ucsd.edu

sequence change in 10 amino acids and truncation of the last 22 amino acids. Although *esa1-414* cells have a growth rate similar to wild type at 30°, they are sensitive to DNA damage (Chang and Pillus 2009). The phenotypes of *esa1-414* cells can be exacerbated by growth at elevated temperatures, conditions under which histone H4 acetylation is decreased and cells slow and/or stop growth by blocking cell cycle progression in G2/M (Clarke *et al.* 1999; Chang and Pillus 2009).

To oppose acetylation, *Saccharomyces cerevisiae* expresses three class I HDACs (Rpd3, Hos2, and Hos1), two class II HDACs (Hda1 and Hos3) (Yang and Seto 2008), and five class III HDACs or Sirtuins, including Sir2, Hst1, Hst2, Hst3, and Hst4 (Brachmann *et al.* 1995; Frye 2000). Rpd3 is active in two different complexes, Rpd3S and Rpd3L (Figure 1A), both of which deacetylate histones H3, H4, H2A, and H2B (Shahbazian and Grunstein 2007; Rando and Winston 2012), as well as many nonhistone proteins (Carrozza *et al.* 2005a,b; Keogh *et al.* 2005). Both complexes share a core defined by the Rpd3, Sin3, and Ume1 subunits (Carrozza *et al.* 2005b; Chen *et al.* 2012). Rpd3L is required for stress response and transcriptional silencing (Zhou *et al.* 2009; Ruiz-Roig *et al.* 2010). The Sds3, Dep1, Cti6, Sap30, Rxt2, Rxt3, and Pho23 subunits, in combination with the Rpd3 core, form the Rpd3L complex that is recruited to gene promoters by Ume6 and Ash1 subunits (Carrozza *et al.* 2005a; Zhou *et al.* 2009; Ruiz-Roig *et al.* 2010). The Rpd3S complex is formed by the Rpd3 core and the Eaf3 and Rco1 subunits (Carrozza *et al.* 2005b). Rpd3S is directed by Eaf3 to methylated histone H3K36, predominantly found at the 3′ end of coding regions, to repress cryptic transcription (Carrozza *et al.* 2005b). Rpd3 was recently reported in a third complex, Rpd3μ, along with the Snt2 and Ecm5 subunits (Figure 1A) (Shevchenko *et al.* 2008; McDaniel and Strahl 2013). This complex is enriched at promoter regions and has a role in the response to oxidative stress (Baker *et al.* 2013), but little else is yet known about its function.

Genetic, biochemical, and genome-wide studies suggest that Rpd3 and Hda1 are the most relevant opposing activities to Esa1 (Vogelauer *et al.* 2000; Lin *et al.* 2008; Chang and Pillus 2009); yet important questions remain. Rpd3 has been directly identified as the deacetylase for some histone and nonhistone targets of Esa1 (Lu *et al.* 2011; Rando and Winston 2012; Yi *et al.* 2012), whereas genetic interaction networks point to deletion of *HDA1* as the most prominent alleviating hub for NuA4 (Lin *et al.* 2008). Hda1 also has some overlapping functions with Rpd3 (Bernstein *et al.* 2000; Robyr *et al.* 2002). Finally, even though strong hypomorphic alleles of *ESA1* have been studied (Clarke *et al.* 1999; Decker *et al.* 2008; Lin *et al.* 2008), residual Esa1 activity could mask the discovery of *esa1*Δ phenotypes. In this work we define the Rpd3L complex as the relevant opposing activity to Esa1's essentiality through the identification of a gene deletion that allows *ESA1* null cells to live. This bypass suppression validates and extends previous suggestions about the need for a balanced acetylation status for viability (Zhang *et al.* 1998; Lin *et al.* 2008). Importantly, however, we also demonstrate that modulation of acetylation states through specific genetic interventions can restore essential functions required for growth, cell cycle progression, and response to DNA damage and stress.

Materials and Methods

Yeast strains and plasmids

Yeast strains, plasmids, and oligonucleotides are listed in Supporting Information, Table S1, Table S2, and Table S3. The *esa1-414* allele (Clarke *et al.* 1999) and the *hst1*Δ*2*::*LEU2* gene disruption (Smith *et al.* 2000)—for simplicity referred to herein as *hst1*Δ—were previously described. All other mutants are null alleles constructed with standard methods. *hst1*Δ (Smith *et al.* 2000) was introduced into the W303 background by amplification of the *LEU2* cassette from strain YCB232. The *rpd3*Δ::*LEU2* (DY1539), *hda1*Δ::*TRP1* (DY4891), and *hos2*Δ::*TRP1* (DY4549) parental strains were all generous gifts from D. Stillman. The parental *sap30*Δ::*kanmx* strain (MAY8) was a generous gift from J. Heitman, and *dep1*Δ::*HIS3* (YJW678) was kindly provided by J. Workman. Silencing reporter and histone mutant strains were constructed as described (Chang and Pillus 2009), starting with strains developed in Roy and Runge (2000). All double and triple *esa1*Δ mutant strains were constructed with a covering plasmid (pLP796). All *esa1*Δ strains were further backcrossed to wild type to assess the tetrad segregation pattern, ruling out possibilities of aneuploidy or additional unlinked suppressors.

Growth assays

Dilution assays were performed as described (Chang and Pillus 2009) with fivefold serial dilutions from A_{600} units of 5 ODs for 5-FOA counterselection assays and of 0.5 ODs for all other media. Camptothecin (CPT) sensitivity was assayed using 7 μg/ml in DMSO, added to YPAD (YPD plus adenine) plates buffered with 100 mM potassium phosphate to pH 7.5 (Nitiss and Wang 1988). The *esa1*Δ *sds3*Δ strains were extremely sensitive to standard concentrations of hydroxyurea (HU) (0.1–0.2 M) and CPT (20–30 μg/ml). They were also sensitive to the CPT solvent, DMSO (0.4%). For this reason, their growth was tested in less concentrated drug and solvent control plates (0.14%). The nature of the DMSO sensitivity has not been established (Zhang *et al.* 2013). UV damage was evaluated as described (Hampsey 1997). Images were captured after 2–5 days of growth.

Flow cytometry

Flow cytometry was done as described in Chang *et al.* (2012). Cells were fixed after growth at 30° on YPAD. A total of 30,000 propidium iodide-stained cells of each strain were analyzed with a FACSCalibur (BD).

Immunoblots

Whole-cell extracts were prepared by bead beating (Clarke *et al.* 1999). Nuclear fractions were prepared as in Kizer

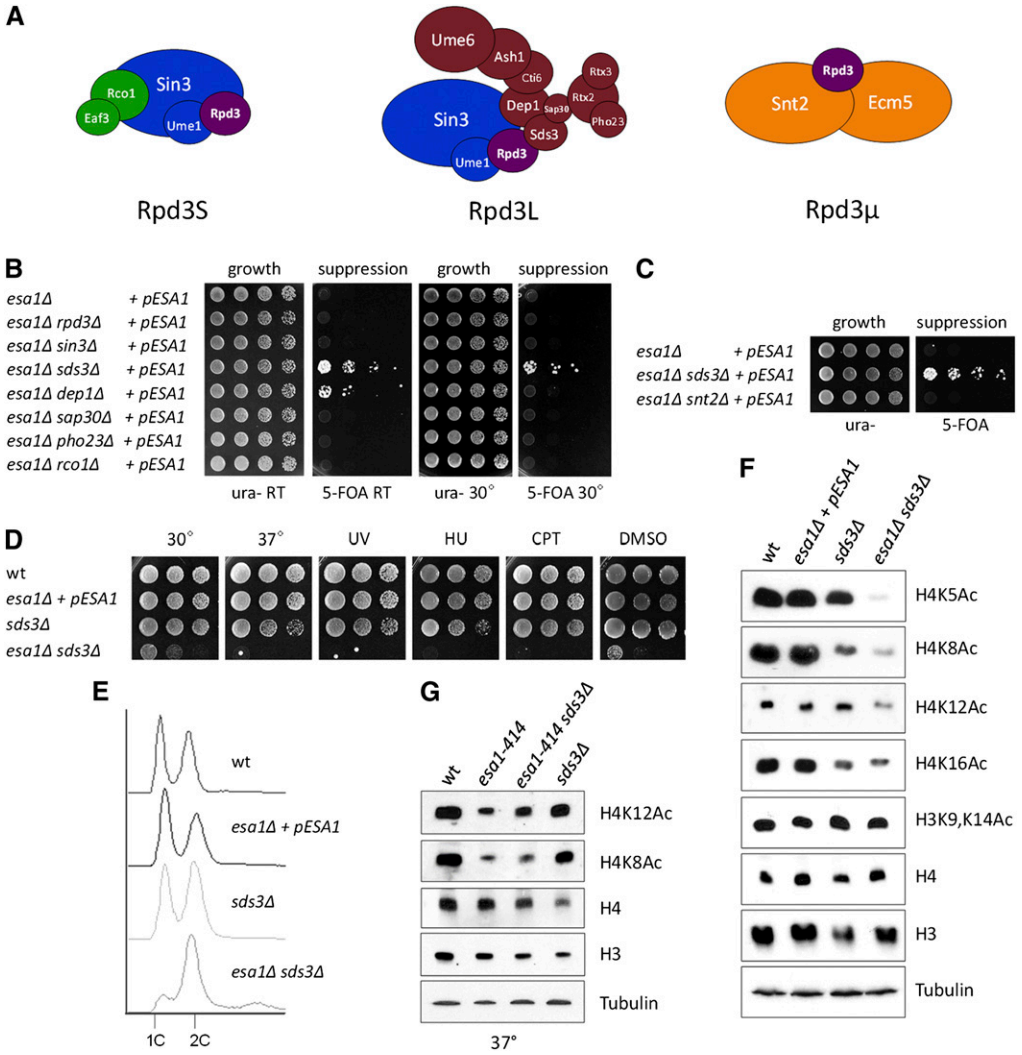

Figure 1 Disruption of Rpd3L bypassed the essential requirement for *ESA1*. (A) Functional organization of Rpd3 complexes with subunits shown to relative scale (adapted from Sardiu *et al.* 2009; McDaniel and Strahl 2013). Loss of *RCO1* disrupts Rpd3S, whereas *SDS3* or *DEP1* deletions disrupt Rpd3L. Deletion of *SNT2* disrupted Rpd3μ. (B) The *esa1*Δ *sds3*Δ and *esa1*Δ *dep1*Δ strains could lose the covering *ESA1* plasmid at room temperature (RT), whereas only the *SDS3* deletion bypassed *esa1Δ* at 30°. Serial dilutions of *ESA1* (*URA3*)-covered strains: *esa1*Δ (LPY12205), *esa1*Δ *rpd3*Δ (LPY12207), *esa1*Δ *sin3*Δ (18032), *esa1*Δ *sds3*Δ (LPY16480), *esa1*Δ *dep1*Δ (LPY20385), *esa1*Δ *sap30*Δ (LPY20465), *esa1*Δ *pho23*Δ (LPY17027), and *esa1*Δ *rco1*Δ (LPY17029). Strains were grown on medium without uracil or with 5-FOA (2 mg/ml). An assay including a wild-type control is shown in Figure S1A. (C) Deletion of *SNT2* was not a bypass suppressor of *esa1*Δ. Assay as in Figure 1B, including *ESA1* covered *esa1*Δ *snt2*Δ (LPY20664). (D) The *esa1*Δ *sds3*Δ strain was temperature and DNA damage sensitive. Four strains were assayed: wild type (LPY79), *esa1*Δ + p*ESA1* (12205), *sds3*Δ (LPY12959), and *esa1*Δ *sds3*Δ (LPY16595). Serial dilutions compared growth at 30°, 37°, and in response to UV light (60 J/m^2) and the drugs HU (0.05 M) and CPT (7 μg/ml dissolved in DMSO). (E) Cell cycle profiles showed that the DNA content of the majority of the *esa1*Δ *sds3*Δ cells was in the 2C peak, indicative of a severe delay in progression through the G2/M phase of the cell cycle. (F) All tested acetylable lysine residues of the histone H4 N-terminal tail had low global levels of acetylation in the *esa1*Δ *sds3*Δ background. Protein extracts were immunoblotted against the isoform or protein-specified. (G) Deletion of *SDS3* improved histone H4K8 and K12 acetylation when *esa1-414* was inactivated by growth at 37°. See Figure S1, B and C, for quantification of immunoblots.

et al. (2006). Proteins were transferred to PVDF membranes (Hybond) and probed with the following: anti-H4K5Ac (1:5000 dilution, Serotec), anti-H4K8Ac (1:2000 dilution, Serotec), anti-H4K12Ac (1:2000 dilution, Active Motif), anti-H4K16Ac (1:2000 dilution, Upstate), anti-H3CT (1:10,000 dilution, Millipore), anti-H3K9,K14Ac (1:10,000 dilution, Upstate), anti-H4 (1:2000 dilution, Active Motif), and anti-β-tubulin (1:20,000) (Bond *et al.* 1986). All antisera except H4 were diluted in 2.5% milk in TBS–Tween. Anti-H4 was diluted in 5% BSA in TBS–Tween. Experiments were performed independently from two to five times.

Immunoblot quantification

Two to five independent experiments were quantified using the ImageQuant 5.2 program (Molecular Dynamics). The histogram peak function was applied to correct for background.

Plasmid end-joining assay

Assays with pRS316 were performed with established methods (Åström *et al.* 1999; Lee *et al.* 1999). Four independent experiments were performed, and *P*-values were calculated using the Student's *t*-test.

Recombination assays

Performed as described (Clarke *et al.* 2006). Approximately 5000 colonies per isolate were counted in four independent experiments. When strains lost the *rDNA*::*ADE2 CAN1* marker inserted in the repetitive rDNA array, they became adenine auxotrophs and developed red pigment sectors. The number of half-red sectored colonies divided by the total number of colonies plated reported the frequency of cells in a population that had undergone a recombination event during the first cell division. The Student's *t*-test was applied to assess significance.

DNA silencing assay

Expression of the *CAN1* gene integrated in the rDNA cluster was detected as canavanine sensitivity when silencing was compromised (16 mg/ml) (Chang and Pillus 2009).

Results and Discussion

The discovery that *ESA1* is an essential gene was significant because prior studies of single mutants of other HATs and HDACs had revealed important roles in gene expression, but not a role in viability. The powerful tool of genetic suppression has facilitated the characterization of conditional, non-null alleles of *ESA1* (Biswas *et al.* 2008; Lin *et al.* 2008; Chang and Pillus 2009; Scott and Pillus 2010; Chang *et al.* 2012); however, much remains to be learned about its cellular roles.

Bypassing the requirement for an essential acetyltransferase

Although a condition bypassing the essential function of *ESA1* has been alluded to in the literature (Natsume-Kitatani *et al.* 2011), its specific molecular identity has not been reported. Deletion of *RPD3* is to date the best suppressor reported for *esa1* alleles (Chang and Pillus 2009), yet *rpd3*Δ cannot bypass *ESA1* since the *esa1*Δ *rpd3*Δ mutant is inviable (Chang and Pillus 2009). As Rpd3 is the catalytic subunit of both Rpd3L and S complexes, we asked if loss of components of either complex would eliminate the need for *ESA1* while maintaining *RPD3* and the activity that it encodes.

Double mutants were constructed, combining *esa1*Δ with deletions of specific subunits of the Rpd3L and Rpd3S complexes (Figure 1A), with the aid of an *ESA1* wild-type gene borne on a *URA3* plasmid. The gene deletions tested included *SDS3*, *DEP1*, *SAP30*, and *PHO23*, all complex-specific subunits of Rpd3L (Lechner *et al.* 2000); *RPD3*, the catalytic subunit of both complexes; *SIN3*, an Rpd3 core subunit; and *RCO1*, a specific subunit of Rpd3S (Carrozza *et al.* 2005a,b; Keogh *et al.* 2005). *SDS3* and *DEP1* deletions disassemble Rpd3L, whereas Rpd3S integrity is lost when *RCO1* is deleted. Neither Pho23 nor Sap30 is essential for the stability of Rpd3L. Strains were tested for growth on 5-FOA, a compound toxic to cells expressing the *URA3* gene marking the *ESA1* plasmid. Growth of a double mutant indicated that the strain could live without the *ESA1* plasmid and thus that the second mutation bypassed *esa1*Δ's lethality. Of the mutants tested, both *SDS3* and *DEP1* deletions bypassed the need for the covering *ESA1* gene (Figure 1B). Thus, the Rpd3L complex opposes the essential function of *ESA1*, resulting in viable cells when both *ESA1* and *SDS3* (or *DEP1*) are deleted. Notably, bypass suppression was not seen upon deletion of *PHO23* or *SAP30*, which encode more peripheral subunits of Rpd3L. Using the same approach, we also found that loss of the Rpd3μ complex (Figure 1A), through deletion of *SNT2* (Baker *et al.* 2013), did not bypass *esa1*Δ (Figure 1C). In further characterization of bypass conditions, we focused on the *SDS3* deletion as it proved to be a stronger suppressor of *esa1*Δ than *dep1*Δ (Figure 1B).

To determine if the *SDS3* deletion suppressed phenotypes that had been defined for *ESA1* alleles, the *esa1*Δ *sds3*Δ strain was evaluated for temperature sensitivity, DNA damage sensitivity, and cell cycle control. In these assays, the *esa1*Δ *sds3*Δ cells grew weakly at 30° and were severely temperature sensitive at 37° (Figure 1D). They were also sensitive to DNA damage induced by UV irradiation and by HU and CPT, compounds that induce DNA DSBs through distinct mechanisms (Figure 1D). The *esa1*Δ *sds3*Δ cells also proved to be sensitive to the DMSO solvent for CPT, mirroring sensitivity reported for other chromatin regulators (Zhang *et al.* 2013).

Flow cytometry revealed that whereas the *sds3*Δ and the *esa1*Δ+*pESA1* strains had a cell cycle profile similar to wild type, the *esa1*Δ *sds3*Δ strain grown at 30° showed a severe delay in progression through G2/M. The severity of this delay reflects the complete loss of *ESA1*, combined with the lack of the Rpd3L complex, which is also involved in cell cycle progression (Bernstein *et al.* 2000; Kaluarachchi *et al.* 2012) (Figure 1E).

To test the hypothesis that *sds3*Δ suppressed *esa1*Δ by restoring isoform-specific acetylation of Esa1 histone targets, whole-cell extracts were analyzed by immunoblotting (Figure 1F). When compared to wild-type strains, low acetylation levels were found for histone H4-modified lysines (Figure 1F). In contrast, acetylation levels of H3, primarily acetylated by other HATs such as Gcn5 and Sas3, remained relatively unaffected (Figure 1F). Notably, several independent *esa1*Δ *sds3*Δ strains constructed in the BY and W303 backgrounds had similar phenotypes. Thus, although *sds3*Δ could bypass the requirement for *ESA1* for viability, the double mutant nonetheless had exacerbated phenotypes previously established for alleles of *ESA1* in cell cycle control and H4 acetylation.

Based on the findings in Figure 1, we hypothesized that deletion of *ESA1* caused a lethal global acetylation imbalance, since histone H3 acetylation levels remained high compared to those of H4 (Figure 1F). When *SDS3* was deleted in combination with *ESA1*, this imbalance was partially alleviated because the Rpd3L complex did not further deacetylate the sparsely acetylated H4. This condition generated slightly higher H4 acetylation levels compared to those predicted for *esa1*Δ that allowed cells to live. As it was unlikely that the global histone acetylation balance in *esa1*Δ *sds3*Δ cells was fully restored, cell fitness remained seriously compromised.

Because the *SDS3* deletion alone did not increase global H4 acetylation (Figure 1F), we took advantage of a strain expressing the *esa1-414* conditional allele to test if loss of Rpd3L affected H4 acetylation in the absence of *ESA1*. The *esa1-414* and *esa1-414 sds3Δ* strains were grown at 37° to further diminish esa1-414's catalytic activity. Figure 1G shows that, when the *SDS3* gene was deleted, the low levels

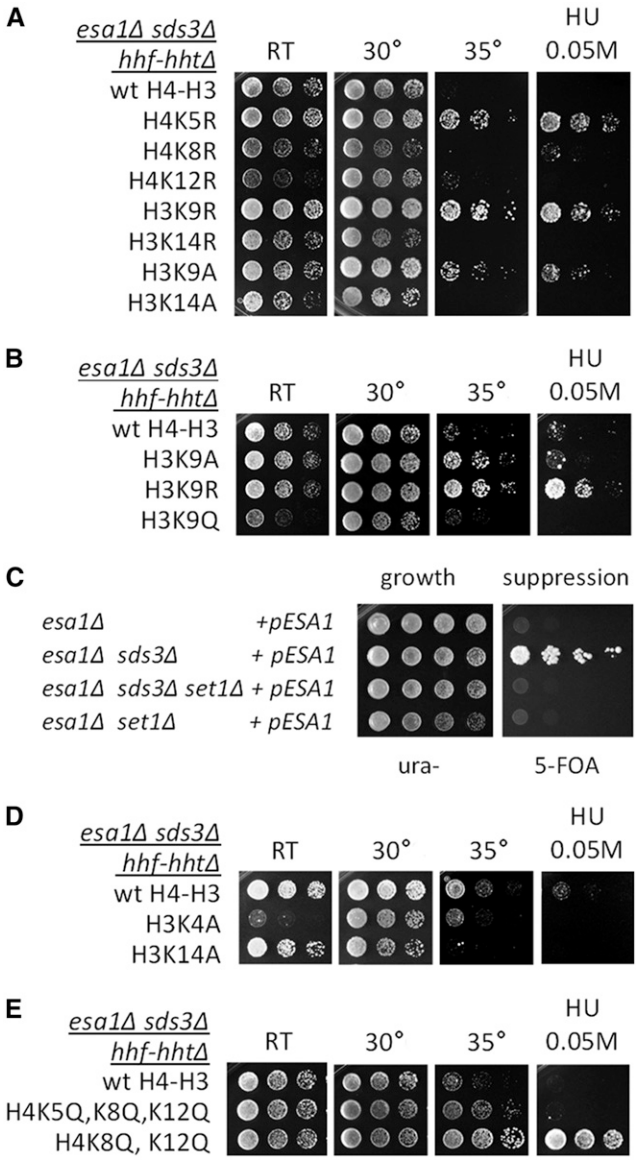

Figure 2 Mutation of histone residues enhanced *esa1*Δ *sds3*Δ fitness. (A) The H3K9R mutant suppressed *esa1*Δ *sds3*Δ temperature and DNA damage sensitivity. An *esa1*Δ *sds3*Δ strain was constructed in which all copies of genes encoding H3 and H4 were deleted *(hht-hhf*Δ) and covered with pJH33 (Ahn *et al*. 2005). Strains shown carried a plasmid either with wild-type H3 and H4 or with one mutated lysine in H4 or H3 as indicated. Lysines were mutated to arginine (R) as an unacetylated lysine mimic, to glutamine (Q) to mimic acetylation, or to alanine (A) as a non-acetylable residue. Plasmid retention was required for survival. Wild-type histones H3-H4 (LPY17368), H4K5R (LPY20430), H4K8R (LPY20431), H4K12R (LPY20432), H3K9R (LPY20388), H3K14R (LPY20389), H3K9A (LPY20387), and H3K14A (LPY20437) in the *esa1*Δ *sds3*Δ *hht1-hhf1*Δ *hht2-hhf2*Δ background were tested in serial dilutions. Hydroxyurea plates were grown at 30°. Strains were very sensitive to DMSO, the solvent for CPT, and thus this drug challenge is not shown (see text). (B) The H3K9Q mutant that mimics highly acetylated H3 in the *esa1*Δ *sds3*Δ background was sick. Serial dilution assays as above compared with the H3K9Q (LPY20661) mutant. (C) *SET1* was required for survival of *esa1Δ* and *esa1Δ sds3Δ* in the absence of p*ESA1*. Assay was as in Figure 1B testing *esa1Δ sds3Δ set1Δ* (LPY20775) and *esa1Δ set1Δ* (LPY20776) strains. (D) Lysine 4 of H3 was critical in the *esa1Δ sds3Δ*. The *esa1Δ sds3Δ* H3K4A mutant (LPY20903) was tested. (E) H4 acetylation mimics in *esa1*Δ *sds3*Δ strains were healthier than those expressing wild-type histones. Tested strains were H4K5Q, K8Q, K12Q (LPY20436) and H4K8Q, K12Q (LPY20435) in the *esa1*Δ *sds3*Δ *hht1-hhf1*Δ *hht2-hhf2*Δ background. Control assays demonstrating no effects on wild-type strains with the histone mutants are shown in Figure S2B.

of histone H4 acetylation were somewhat increased relative to *esa1-414*. This confirmed that deletion of *SDS3* could promote higher acetylation of histone H4 in the absence of *ESA1*.

*Critical histone residues that enhance esa1*Δ *sds3*Δ *fitness*

To test the hypothesis that imbalanced acetylation interfered with the vitality of the *esa1*Δ *sds3*Δ strain, we sought to identify conditions that enhanced fitness. Initially, *esa1*Δ *sds3*Δ strains in combination with histone H4 and H3 lysine (K) to arginine (R) or alanine (A) mutations were constructed and analyzed (Figure 2A and Figure S2A). The arginine mutants were used to retain the positive charge of deacetylated lysines, whereas the alanine mutants were used as non-acetylable residues. Among the mutants, the H3K9R was the best suppressor of *esa1*Δ *sds3*Δ temperature and damage sensitivities (Figure 2A). We had earlier observed that the H3 acetylation levels remained high in *esa1*Δ *sds3*Δ cells (Figure 1F). Thus, it appeared that, if H3K9 cannot be acetylated due to the K-to-R mutation, the global acetylation imbalance can be eased, leading to improved growth under stress conditions. To pursue this idea, an *esa1*Δ *sds3*Δ H3K9Q mutant strain was tested as a proxy for cells with highly acetylated histone H3 in a low-H4-acetylation context. Indeed, this strain proved to be even sicker than cells with wild-type H3 and H4 (Figure 2B).

In contrast to the H3K9 mutants, the H3K14R and A mutants remained sick (Figure 2A), a result that initially appeared at odds with the central importance of balanced histone acetylation. However, H3K14, but not K9, has a more widespread role in transcriptional regulation by interacting with the Jhd2 histone demethylase (Maltby *et al.* 2012). The H3K14A/R mutants result in loss of histone H3K4 trimethylation (Nakanishi *et al.* 2008), a modification that has a direct impact on chromatin structure through the recruitment of modifiers containing methyl-binding domains. Confirming the critical role of H3K4me in the *esa1Δ sds3Δ* strain, *SET1*, the gene encoding the H3K4 methyltransferase (Krogan *et al.* 2002), could not be deleted (Figure 2C) and the H3K4A mutant grew more slowly than the H3K14A mutant in *esa1Δ sds3Δ* cells (Figure 2D).

The H4K5R mutant partially suppressed the temperature and DNA damage sensitivity of the *esa1*Δ *sds3*Δ strain. This result may be considered relative to distinct roles of the Rpd3L and S complexes. Rpd3L is targeted to specific promoter regions (Carrozza *et al.* 2005a), whereas Rpd3S activity is more localized to coding regions by the H3K36-methyl mark from Set2 (Carrozza *et al.* 2005b; Drouin *et al.* 2010; Govind *et al.* 2010). The *esa1*Δ *sds3*Δ strains

are expected to have lower acetylation at gene-coding regions, compared to promoter regions, since Rpd3S remains active in these cells. The H4K5R mutant may thus create a homogeneous non-acetylated H4K5 state that is less deleterious. Acetylation of H4K5, -8, and -12 is considered to be somewhat redundant (Dion *et al.* 2005); nonetheless, the major target of Esa1 acetylation is K5 of H4 (Smith *et al.* 1998; Clarke *et al.* 1999) (Figure 1F). Indeed, the H4K5R mutant was a good suppressor of *esa1*Δ *sds3*Δ whereas the H4K8R and K12R mutants remained sick. Finally, when H4K8 and K12 were simultaneously mutated to glutamine to mimic higher H4 acetylation levels, the *esa1*Δ *sds3*Δ temperature and damage phenotypes were rescued (Figure 2E).

*HDAC deletions can improve esa1*Δ *sds3*Δ *fitness and acetylation*

As a counterpoint to the site mutant studies, we asked if individual HDAC deletions could improve fitness of the *esa1*Δ *sds3*Δ strain. In this case, triple mutants were constructed with select members of each of the three HDAC classes. As before, the mutants were constructed using the covering *ESA1* plasmid, followed by the 5-FOA challenge for plasmid loss (Figure 3A). Furthermore, to test if the Rpd3S complex could be lost after Rpd3L was eliminated, the integral Rpd3S-specific subunit *RCO1* (Carrozza *et al.* 2005b) was also deleted (Figure 3A). Additional deletion of *RPD3* or *RCO1* led to inviability, consistent with the observation that the Rpd3S complex activity is necessary to bypass *esa1*Δ. Deletion of *HOS2* also interfered with bypass suppression, suggesting a significant role for *HOS2* or the Set3 complex (Pijnappel *et al.* 2001) in *esa1*Δ *sds3*Δ. In contrast, three of the HDAC triple mutants grew without the *ESA1* gene. These were *esa1*Δ *sds3*Δ strains with deletions of genes encoding the type II HDAC Hda1 and the Sirtuins Sir2 and Hst1.

When comparing global histone acetylation of *esa1*Δ *sds3*Δ and *esa1-414* cells grown at 34° to partially inactivate Esa1, decreased H4 acetylation was observed in *esa1*Δ *sds3*Δ (Figure 3B). Acetylation increased at all H4 residues tested in the *esa1*Δ *sds3*Δ *hst1*Δ strain (Figure 3B). Compared to *esa1*Δ *sds3*Δ, the *esa1*Δ *sds3*Δ *hda1*Δ strain also showed higher acetylation of H4 except at H4K16. The *esa1*Δ *sds3*Δ *sir2*Δ strain had higher levels of H4K16 acetylation relative to *esa1*Δ *sds3*Δ; however, acetylation of H4K8 and K12 remained low (Figure 3B) with similar results obtained for both whole-cell lysates and isolated nuclei (not shown).

Specific contributions of individual HDACs in diverse cellular functions

Because the patterns of acetylation and overall growth differed among the triple-mutant combinations, we tested the idea that they might have distinct responses to specific cellular challenges. Notably, the *HDA1* deletion improved high temperature growth at 34° and 37° (Figure 4A) and suppressed the cell cycle G2/M block of *esa1*Δ *sds3*Δ (Figure 4B). Loss of *HDA1* also suppressed defective rDNA silencing of *esa1*Δ *sds3*Δ (Figure 4C).

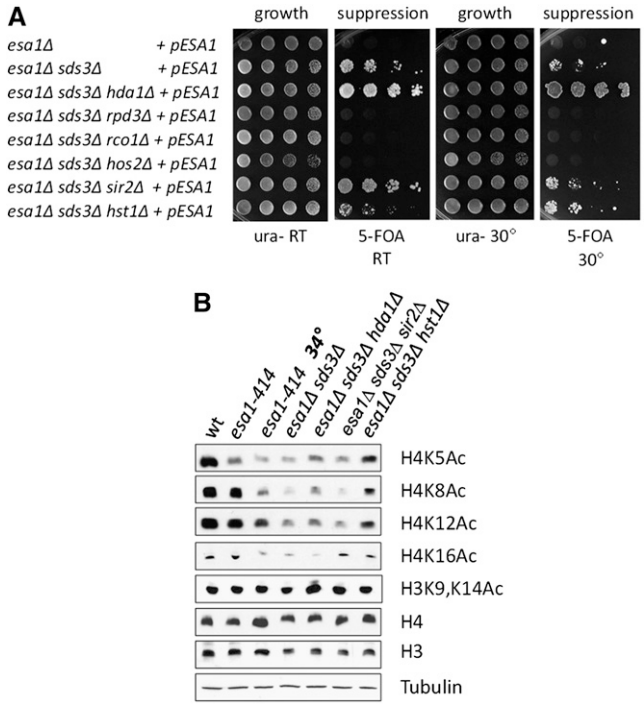

Figure 3 Distinct functional interactions of *esa1Δ sds3Δ* with HDAC deletions. (A) Mutant strains expressing wild-type *ESA1* from a *URA3* vector were challenged on 5-FOA plates using serial dilutions to test for loss of the *URA3* plasmid at RT and 30°. The *esa1*Δ *sds3*Δ strains mutated for *HDA1*, *SIR2*, or *HST1* survived. In contrast, the bypass suppressor strain lost viability upon deletion of *RPD3*, *RCO1*, or *HOS2*, thereby demonstrating specificity for balancing of HDAC activities. Note that the added suppression of *esa1*Δ *sds3*Δ by additional HDAC deletions was strictly dependent on loss of *SDS3* as the corresponding *esa1*Δ HDACΔ mutants were inviable (Figure S3A). The surviving triple mutants could also cure additional *esa1*Δ *sds3*Δ phenotypes (see Figure 4 and Figure 5). Strains tested were *esa1*Δ (LPY12205), *esa1*Δ *sds3*Δ (LPY16480), *esa1*Δ *sds3*Δ *hda1*Δ (LPY17759), *esa1*Δ *sds3*Δ *rpd3*Δ (LPY 17714), *esa1*Δ *sds3*Δ *rco1*Δ (LPY17805), *esa1*Δ *sds3*Δ *hos2*Δ (LPY17848), *esa1*Δ *sds3*Δ *sir2*Δ (LPY17966), and *esa1*Δ *sds3*Δ *hst1*Δ (LPY17801). (B) Different HDACs improved acetylation at specific histone H4 residues. Extracts from strains in A without the *ESA1* plasmid were probed for lysine-specific modifications. Additional controls included wild-type and *esa1-414* strains. The *esa1-414* strain was also grown at 34° to partially inactivate esa1-414. Strains tested were wild type (LPY79), *esa1-414* (LPY4776), *esa1*Δ *sds3*Δ (LPY16595), *esa1*Δ *sds3*Δ *hda1*Δ (LPY17748), *esa1*Δ *sds3*Δ *sir2*Δ (LPY17997), and *esa1*Δ *sds3*Δ *hst1*Δ (LPY17900). Quantification of blots is shown in Figure S3, B and C. Histone H3 levels were modestly decreased in all bypass strains, whereas H4 levels remained relatively unaffected. The nature of the change of histone levels is not established; however, precedents for specific changes in histone levels have been reported under a variety of physiological or signaling conditions (Dang *et al.* 2009; Feser *et al.* 2010; Turner *et al.* 2010). In particular, loss of the Asf1 chaperone and other conditions leading to a G2/M block have been associated with decreased histone H3 levels (Feser *et al.* 2010).

The immunoblot results in Figure 3B show that Hda1 opposed Esa1 function by deacetylating H4, whereas H3 acetylation remained high, as Hda1 is largely an H3 deacetylase. The same results were found at elevated temperatures (Figure 4D). Hda1 might oppose *ESA1* function at overlapping Rpd3L targets that include cell cycle genes by

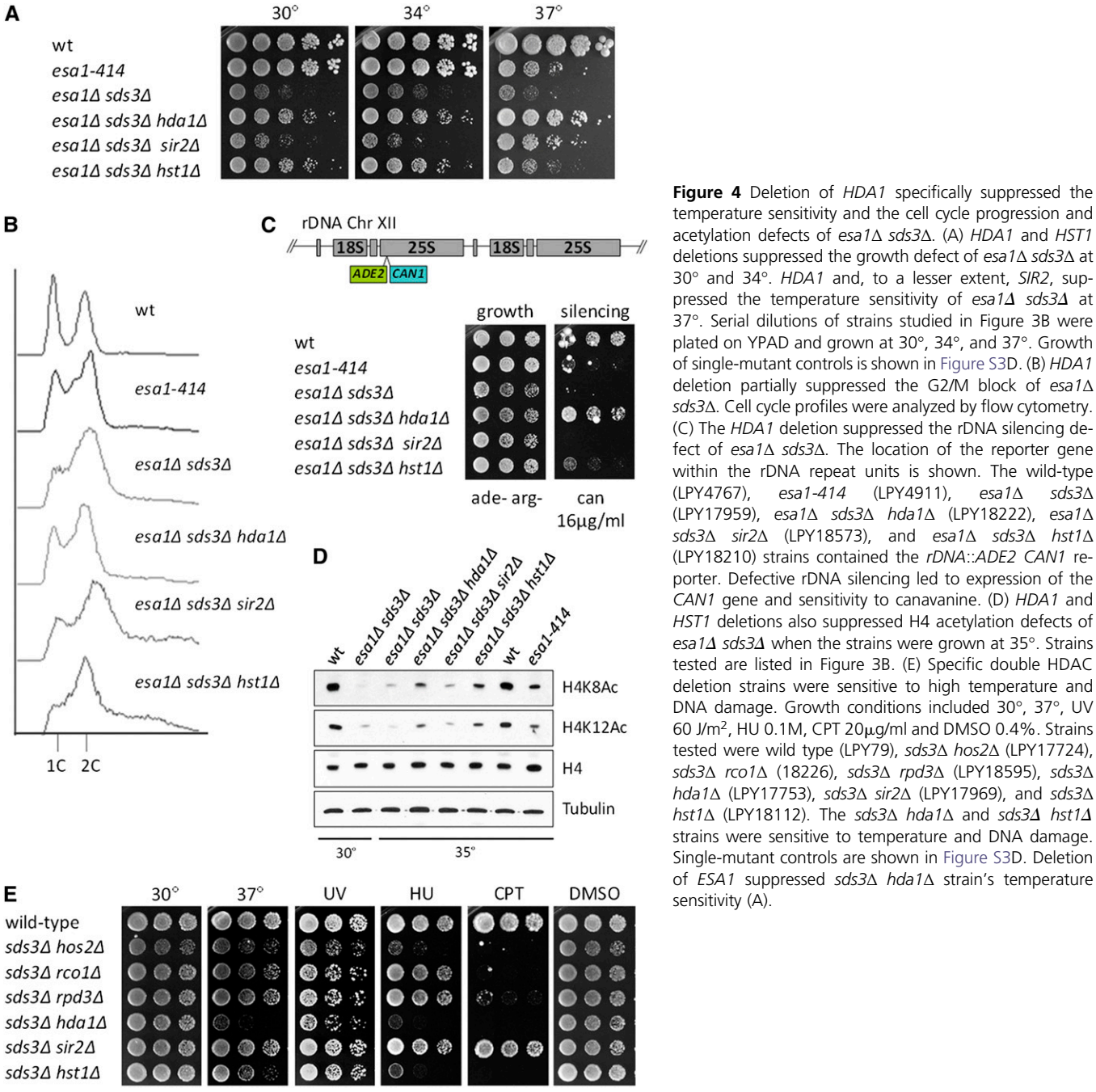

Figure 4 Deletion of *HDA1* specifically suppressed the temperature sensitivity and the cell cycle progression and acetylation defects of *esa1*Δ *sds3*Δ. (A) *HDA1* and *HST1* deletions suppressed the growth defect of *esa1*Δ *sds3*Δ at 30° and 34°. *HDA1* and, to a lesser extent, *SIR2*, suppressed the temperature sensitivity of ***esa1Δ sds3Δ*** at 37°. Serial dilutions of strains studied in Figure 3B were plated on YPAD and grown at 30°, 34°, and 37°. Growth of single-mutant controls is shown in Figure S3D. (B) *HDA1* deletion partially suppressed the G2/M block of *esa1*Δ *sds3*Δ. Cell cycle profiles were analyzed by flow cytometry. (C) The *HDA1* deletion suppressed the rDNA silencing defect of *esa1*Δ *sds3*Δ. The location of the reporter gene within the rDNA repeat units is shown. The wild-type (LPY4767), *esa1-414* (LPY4911), *esa1*Δ *sds3*Δ (LPY17959), *esa1*Δ *sds3*Δ *hda1*Δ (LPY18222), *esa1*Δ *sds3*Δ *sir2*Δ (LPY18573), and *esa1*Δ *sds3*Δ *hst1*Δ (LPY18210) strains contained the *rDNA*::*ADE2 CAN1* reporter. Defective rDNA silencing led to expression of the *CAN1* gene and sensitivity to canavanine. (D) *HDA1* and *HST1* deletions also suppressed H4 acetylation defects of ***esa1Δ sds3Δ*** when the strains were grown at 35°. Strains tested are listed in Figure 3B. (E) Specific double HDAC deletion strains were sensitive to high temperature and DNA damage. Growth conditions included 30°, 37°, UV 60 J/m^2, HU 0.1M, CPT 20μg/ml and DMSO 0.4%. Strains tested were wild type (LPY79), *sds3*Δ *hos2*Δ (LPY17724), *sds3*Δ *rco1*Δ (18226), *sds3*Δ *rpd3*Δ (LPY18595), *sds3*Δ *hda1*Δ (LPY17753), *sds3*Δ *sir2*Δ (LPY17969), and *sds3*Δ ***hst1Δ*** (LPY18112). The *sds3*Δ *hda1*Δ and ***sds3Δ hst1Δ*** strains were sensitive to temperature and DNA damage. Single-mutant controls are shown in Figure S3D. Deletion of *ESA1* suppressed *sds3*Δ *hda1*Δ strain's temperature sensitivity (A).

deacetylating histones H3 and H4 (Bernstein *et al.* 2000). It is also possible that Hda1 deacetylates Esa1's nonhistone targets, thus improving overall acetylation levels of these substrates. The chromatin landscape of *esa1*Δ *sds3*Δ *hda1*Δ cells includes higher acetylation of histone H4K5, K8, and K12 compared to *esa1*Δ *sds3*Δ, likely resulting in a more balanced H3/H4 acetylation ratio at target genes important for progression through the cell cycle and silencing. This idea could explain Hda1's prominent role in NuA4 synthetic interaction networks (Lin *et al.* 2008). Lysines 5, 8, and 12 of histone H4 are targets of the same histone-modifying complexes. Therefore, greater acetylation at these residues in the *esa1*Δ *sds3*Δ *hda1*Δ strain are consistent with their proposed overlapping roles in chromatin (Dion *et al.* 2005). H4K16 acetylation had a different and independent role (below).

Deletion of *HST1* promoted restoration of H4 acetylation in *esa1*Δ *sds3*Δ (Figure 3B and Figure 4D). As *HST1* is responsible for sensing and regulating cellular NAD+ levels (Bedalov *et al.* 2003), the *esa1*Δ *sds3*Δ *hst1*Δ strain may have deregulated NAD+ that negatively affects other Sirtuin HDAC functions. Suppression of the acetylation defect correlated with improved growth (Figure 4A), but not with suppression of cell cycle defects (Figure 4B), sensitivity to

DNA damage, or 37° incubation. This suggests that increased H4 acetylation alone is not adequate to promote robust cellular function; perhaps H4 acetylation must instead be localized to specific chromatin regions, or increased acetylation of nonhistone substrates is required to suppress specific *esa1*Δ *sds3*Δ phenotypes.

The complex biology of balancing acetylation is seen further in Figure 4E. In the *sds3*Δ *hda1*Δ double mutant, where Rpd3L and Hda1 HDAC complexes were further disrupted, there was sensitivity to high temperature (Figure 4E). Indeed, the growth of *esa1*Δ was improved in triple mutants with the *sds3*Δ *hda1*Δ and ***sds3Δ hst1Δ*** deletions (Figure 4A), the double mutants of which were by themselves the sickest tested (Figure 4E), underscoring the complex nature of functional interactions between these acetylase and deacetylase activities.

Alleviating esa1Δ sds3Δ DNA damage sensitivity by deleting SIR2

When the triple-mutant strains were tested for DNA damage sensitivity, all HDAC deletions improved growth after UV irradiation (Figure 5A). Similarly, the triple mutants suppressed the extreme DMSO sensitivity of the *esa1*Δ *sds3*Δ strain (Figure 5A). This suppression suggested that the reduced growth in DMSO correlated with a severely affected chromatin state, as deletion of single chromatin regulators has been previously associated with DMSO sensitivity (Zhang *et al.* 2013).

In contrast to uniform improvements in the triple mutants after UV, only the *SIR2* deletion suppressed sensitivity to DSBs induced by CPT and HU (Figure 5A). *SIR2* had been previously linked to the DNA damage response (Tamburini and Tyler 2005; McCord *et al.* 2009), but we further considered that this suppression might also be coupled to the pseudodiploid state in *SIR2* null cells caused by de-repression of the cryptic mating-type loci (Haber 2012).

DSBs can be repaired by either of two pathways: nonhomologous end joining (NHEJ) or homologous recombination (HR) (Chapman *et al.* 2012). NHEJ is error-prone as it predominantly ligates broken DNA ends (Betermier *et al.* 2014), whereas the HR pathway is more accurate as it uses an intact copy of the affected region as a template for repair. The a1-α2 repressor expressed in diploid and *SIR2* null strains represses specific genes involved in the NHEJ pathway (Åström *et al.* 1999; Valencia *et al.* 2001). This is believed to increase HR efficiency, as diploid cells contain a second copy of each chromosome that can be used as a template for repair (Haber 2012). As with *SIR2* null cells, the *esa1*Δ *sds3*Δ *sir2*Δ strain was non-mating, confirming that the cryptic mating loci were not silenced in haploid cells.

To investigate NHEJ repair efficiency, a plasmid religation assay was used. The assay consists of transforming a linearized plasmid and counting the transformants that repaired the linear plasmid to convert it into a circular and thereby stably maintained plasmid (Åström *et al.* 1999; Lee *et al.* 1999). We found that *esa1-414* and *esa1*Δ *sds3*Δ strains had increased NHEJ repair efficiency compared to wild type, one possible reason for their DNA damage sensitivity phenotypes (Figure 5B). Because in endpoint drug challenge assays the ***esa1Δ sds3Δ*** strain was orders of magnitude more sensitive to DNA damage than the *esa1-414* strain (Figure 5A), we suspected that a severely altered chromatin structure in the bypass strain could influence other aspects of the repair process, such as the transcriptional response or the direct repair of the breaks. In contrast, the *esa1*Δ *sds3*Δ *sir2*Δ strain was defective in NHEJ repair to the same extent as *sir2*Δ (Figure 5B). This suggested that the *esa1*Δ *sds3*Δ *sir2*Δ strain had improved growth on CPT and HU because it was essentially repairing by HR, thereby avoiding mutations that could be introduced during the end-joining repair pathway.

SIN3 and *RPD3* null strains are sensitive to DNA damage induced by phleomycin although they are not sensitive to HU, which, like CPT, is an S-phase-specific DSB inducer (Jazayeri *et al.* 2004). Such differential sensitivity is consistent with a role for Rpd3-Sin3 in NHEJ repair. By contrast, *sds3*Δ strains are sensitive to S-phase DSBs (Chang and Pillus 2009), suggesting that Rpd3L has a more prominent role in HR compared to Rpd3 as part of the core complex. This is consistent with our observations. The *esa1*Δ *sds3*Δ strain was very sensitive to CPT and had a higher rate of NHEJ compared to wild type. When the *SIR2* gene was deleted in the *esa1*Δ *sds3*Δ strain, the NHEJ bias was shifted toward HR repair, making these cells resistant to S-phase-induced damage.

In an independent approach we analyzed recombination using reporter strains in which the *ADE2* gene was inserted in the rDNA locus. Expression of *ADE2* produced white colonies; however, chromosomal loss of *ADE2* due to recombination between the rDNA repeats generated sectored red colonies. In quantifying the relative number of half-red-sectored colonies, we found that the *esa1*Δ *sds3*Δ *sir2*Δ strain showed high levels of rDNA recombination (Figure 5C). It is important to note that *sir2*Δ strains have similar high rDNA recombination levels (Gottlieb and Esposito 1989; Clarke *et al.* 2006); however, the high recombination rate is restricted to specific genomic areas (Su *et al.* 2000; Mieczkowski *et al.* 2007). In the *esa1*Δ *sds3*Δ *sir2*Δ strain, the genomic areas susceptible to recombination may be more dispersed than in *sir2*Δ cells as Rpd3 has a role in repressing mitotic recombination (Dora *et al.* 1999; Merker *et al.* 2008).

Finally, to test if the DNA damage resistance of the *esa1*Δ *sds3*Δ *sir2*Δ strain was due to a pseudodiploid state, we transformed a *MAT*α *esa1*Δ *sds3*Δ strain with a plasmid-borne *MAT***a** locus. Enhanced suppression of the DNA-damage-sensitive phenotype was not observed (Figure 5D). This suggested that the DNA-damage-resistant phenotype of *esa1*Δ *sds3*Δ *sir2*Δ cells was not due simply to a pseudodiploid state but was more likely to result from enhanced levels of acetylation of Sir2 substrates, including H4K16 (Figure 3B), which is a mark of open chromatin that is involved in repair (Bird *et al.* 2002; Tamburini and Tyler 2005).

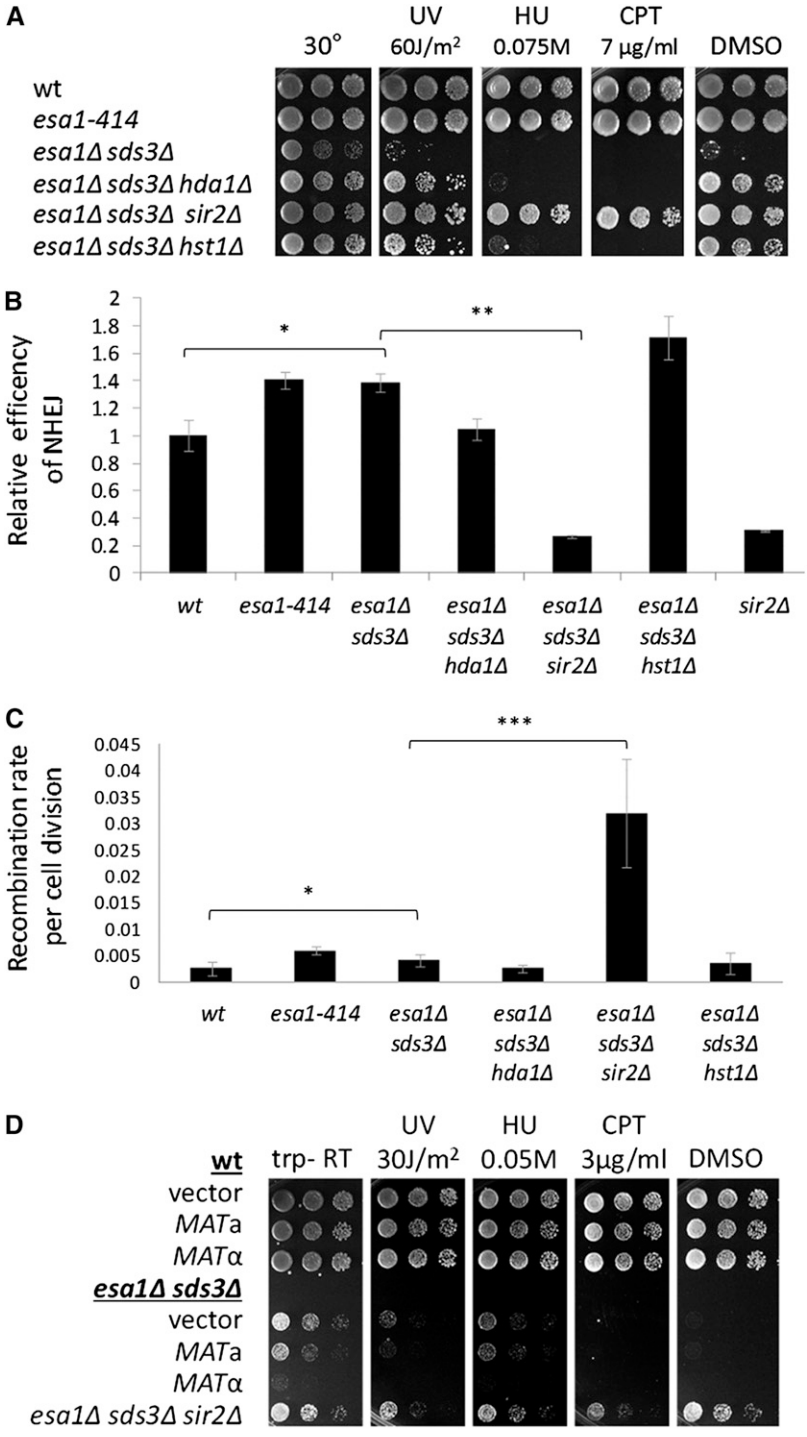

Figure 5 HDAC-specific effects on DNA damage sensitivity and repair. (A) *SIR2* deletion broadly suppressed the DNA damage sensitivity of *esa1*Δ *sds3*Δ. Loss of *HDA1* and *HST1* also suppressed UV and DMSO sensitivity in *esa1*Δ *sds3*Δ. Serial dilutions of strains in Figure 4A were plated on YPAD and DNA damage plates. (B) The *esa1*Δ *sds3*Δ *sir2*Δ mutant down-regulated the NHEJ repair pathway. A plasmid end-joining assay was performed with strains analyzed in A and with *sir2*Δ (LPY18223) as an additional control. Data are expressed as NHEJ efficiency relative to wild type, after normalization to the corresponding transformation efficiency of the uncut plasmid. The repair efficiencies of *esa1-414* and *esa1*Δ *sds3*Δ were identical, but they differed significantly from wild type and *esa1*Δ *sds3*Δ *hda1*Δ ($p = 0.02$), demonstrating that deletion of *HDA1* enhanced NHEJ levels of *esa1*Δ *sds3*Δ. The re-ligation efficiency of *esa1*Δ *sds3*Δ *sir2*Δ was statistically distinct from *esa1*Δ *sds3*Δ ($p < 0.005$), whereas the NHEJ efficiency of *esa1*Δ *sds3*Δ *hst1*Δ was higher than in *esa1*Δ *sds3*Δ ($p = 0.01$), demonstrating that *HST1* deletion led to a further up-regulation of the NHEJ pathway. A previous report found that two different *esa1* hypomorphic alleles had defective NHEJ (Bird *et al.* 2002). Results demonstrating enhanced NHEJ here could be due to allele-specific differences as seen in earlier studies comparing the severity of phenotypic defects and strength of suppression between different *esa1* alleles (Decker *et al.* 2008; Chang *et al.* 2012). (C) The *esa1*Δ *sds3*Δ *sir2*Δ strain had high levels of mitotic recombination in the rDNA array. Recombination was evaluated using a marker-loss assay. The *esa1-414* and *esa1*Δ *sds3*Δ strains had higher recombination rates than wild type ($p < 0.05$); however, *esa1-414* was higher than *esa1*Δ *sds3*Δ ($p = 0.024$). Previous *esa1-414* results were reproduced (Clarke *et al.* 2006). The *esa1*Δ *sds3*Δ *hda1*Δ strain was not distinct from wild type, demonstrating that *HDA1* deletion suppressed the high recombination rates of *esa1*Δ *sds3*Δ ($p = 0.03$). The *esa1*Δ *sds3*Δ *sir2*Δ strain was statistically different from *esa1*Δ *sds3*Δ ($p = 0.0009$), whereas *esa1*Δ *sds3*Δ *hst1*Δ was not. In this case, loss of Rpd3L could not oppose the induced higher rDNA recombination rates in *sir2*Δ deletion, perhaps related to the concomitant *ESA1* loss (Zhou *et al.* 2009) and/or to an Rpd3S-specific function at the rDNA. (D) A pseudodiploid state was not sufficient for DNA damage resistance in *esa1*Δ *sds3*Δ. Wild-type (LPY79) and *esa1*Δ *sds3*Δ (LPY16595) *MAT*α strains were transformed with *TRP1* plasmids encoding the *MAT***a** or *MAT*α locus and the vector alone as a control. The strains were compared to *esa1*Δ *sds3*Δ *sir2*Δ::*TRP1* (LPY17997) under DNA-damage-inducing conditions on trp− plates. Wild-type strains were unaffected by simultaneous expression of both *MAT* genes. The pseudodiploid *esa1*Δ *sds3*Δ strain remained sensitive to DNA damage when compared with the *esa1*Δ *sds3*Δ *sir2*Δ strain, where a pseudodiploid state was combined with global high levels of histone H4K16 acetylation. The slightly exacerbated HU sensitivity of *esa1*Δ *sds3*Δ upon *MAT*α overexpression may relate to the previously reported synthetic lethality of *rpd3*Δ strains when *MAT*α2 was overexpressed (Kaluarachchi *et al.* 2012).

Conclusions

The human MYST gene *TIP60*, like its yeast homolog *ESA1*, is essential for viability (Gorrini *et al.* 2007) and contributes to the DNA damage response through mechanisms that are under active investigation (reviewed in Squatrito *et al.* 2006; Xu and Price 2011). Because of the deeply conserved characteristics of these genes and their other diverse functions, it is important to understand the nature of their essential functions. In this study, we took advantage of the powerful tool of genetic suppression (reviewed in Prelich 1999) to define an imbalance in dynamic acetylation and deacetylation as the factor underlying lethality in *esa1*Δ

mutants. By restoring acetylation through fine-tuning the spectrum of active enzymes in the cell, it was possible to restore viability and successful responses to environmental stressors. It is also likely that keeping acetylation balanced through tight regulation of Tip60 activity is important in human cells, as altered Tip60 levels have been linked to both suppression and promotion of multiple types of cancer (Squatrito *et al.* 2006; Avvakumov and Côté 2007).

Special relationships between Esa1 and HDACs have been pointed to in earlier studies (Biswas *et al.* 2008; Lin *et al.* 2008; Chang and Pillus 2009) along with the discovery of other suppressors (Chang *et al.* 2012). However, none of these suppressors could bypass the need for *ESA1*. There has been some discussion about whether Esa1's catalytic activity is its essential function (Smith *et al.* 1998; Decker *et al.* 2008), and there is structural and proteomic evidence that auto-acetylation and acetylation of nonhistone substrates are major contributors in the requirement for Esa1 (Yan *et al.* 2002; Lin *et al.* 2009; Lu *et al.* 2011; Yi *et al.* 2012). Our observation that the lethality of *esa1Δ* can be bypassed by the loss of a single HDAC complex supports the idea that *ESA1*'s essential function is its catalytic activity. Importantly however, it is that activity in the context of balancing the overall acetylation state of the cell that is critical.

Viability of the *esa1*Δ *sds3*Δ strain added emphasis to previous data implicating a significant functional relationship between Esa1 and Rpd3 (Biswas *et al.* 2008; Chang and Pillus 2009; Lu *et al.* 2011; Yi *et al.* 2012). The best-studied nonhistone targets of Esa1 are also deacetylated by Rpd3 (Lin *et al.* 2008; Lu *et al.* 2011; Yi *et al.* 2012), suggesting that these substrates may be part of an extreme acetylation imbalance that leads to death in *esa1*Δ cells. If nonhistone targets of Esa1 have a role in viability, at least some are also likely to be deacetylated by Rpd3L and consequently remain in a relatively balanced acetylation state in *esa1*Δ *sds3*Δ strains.

Our data support the idea that the inviability in *esa1*Δ cells may be caused in part by disproportionately high H3 acetylation compared to H4 acetylation, which is extremely low due to loss of Esa1, the primary nuclear H4

Figure 6 Bypassing an essential acetyltransferase by balancing dynamic acetylation. (A and B) *ESA1* deletion resulted in a deleterious decrease in acetylation including a high H3:low H4 acetylation ratio. Imbalanced acetylation of nonhistone substrates of Esa1 is also likely to have a role in lethality of *esa1Δ* strains. (C) When the acetylation ratio was balanced by deletion of *SDS3*, *esa1Δ* cells were viable, although still compromised for growth. (D–G) Balancing acetylation of histone and nonhistone substrates to different extents further improved cell fitness and response to specific challenges. A promoter region and a coding region (blue) separated by the transcriptional start point (arrow) are represented for each genetic condition. Histones H2A and H2B are not shown for simplicity; likewise, only one of the tails of H3 and H4 are depicted. Nonhistone substrates are represented as a circle, a triangle, and a pentagon, and their acetylation is shown as red dots.

acetyltransferase (Figure 6, A and B). At the molecular level imbalanced acetylation is likely to influence multiple aspects of chromatin, including nucleosomal integrity, chromosomal stability, or enzymatic complex affinity for genomic targets. However, enhanced histone acetylation could not rescue all *esa1Δ sds3Δ* phenotypes, suggesting that balanced acetylation of both histone and nonhistone substrates of Esa1 is critical for robust growth in the absence of this essential enzyme. Supporting this idea, in proteomic studies >200 nonhistone substrates have been reported for NuA4 (Lin *et al.* 2009; Mitchell *et al.* 2013), and of these, at least 77 are encoded by essential genes. Substrates include components of the chromatin-remodeling complex RSC (*e.g.*, *STH1* and *RSC8*), proteins involved in ribosome biogenesis (*e.g.*, *NOP4* and *DBP6*), and cytoskeleton and spindle components (*e.g.*, *TUB2* and *SPC42*), whose acetylation state and role in viability in *esa1Δ* and *esa1Δ sds3Δ* remain to be tested.

In *esa1*Δ *sds3*Δ cells, because the Rpd3L complex is not present to deacetylate targets shared with Esa1 and other HATs, the need for *ESA1* can be bypassed (Figure 6C). However, the *esa1*Δ *sds3*Δ cells are very sick, a state that can be further improved by manipulating other chromatin modifiers and specific lysines in histones H3 and H4.

The fitness of the *esa1*Δ *sds3*Δ strain improves to differing extents depending on which additional chromatin modifier is affected, and the balancing act can be more or less robust depending on the target genes, chromatin regions regulated by the modifier, and/or histone and nonhistone substrates affected. One example includes a non-acetylable lysine 9 in histone H3 that significantly improved *esa1*Δ *sds3*Δ fitness. In these cells, H3 acetylation levels are lower and more balanced relative to low H4 acetylation (Figure 6D). Another example involves deletion of *HDA1* that encodes a second HDAC, which increases acetylation of H4 and possibly of shared nonhistones substrates with Esa1 (Figure 6E). The *esa1Δ sds3Δ sir2Δ* strain is an example where fitness may additionally be influenced by cell-specific transcription. In this case, a pseudodiploid state is not sufficient, but may help promote error-proof repair of damaged DNA (Figure 6F). Finally, even though the *esa1Δ sds3Δ hst1Δ* strain has an improved H3/H4 acetylation ratio, it is not as fit as the *esa1Δ sds3Δ hda1Δ* strain, suggesting that in *esa1Δ sds3Δ hst1Δ*, acetylation of nonhistone substrates of Esa1 is not adequately balanced (Figure 6G). Together, the interplay of opposing acetylation activities can lead to a critical balance that promotes viability even under circumstances where death would normally result.

Acknowledgments

We thank C. Chang, L. G. Clark, S. Edwards, M. R. Eustice, R. M. Garza, E. Petty, J. Rine, F. Solomon, and B. X. Su for their critical reading of the manuscript; D. Stillman, J. Workman, J. Heitman, and C. Chang for generously providing strains; members of the Pillus lab for helpful advice throughout the course of this study; and N. Frank for discussion and analyzing data on nonhistone substrates of Esa1. M. M. Smith and his colleagues have also independently observed that loss of components of Rpd3L can bypass *esa1*Δ. We appreciate the communication of their unpublished results. This work was initiated with the previous support of National Institutes of Health grant GM5649 and continued with funding from the University of California Cancer Research Coordinating Committee and the University of California at San Diego Committee on Research. A. L.T.-M. was supported by the University of California Institute for Mexico and the United States (UCMEXUS) and the National Council of Science and Technology of Mexico (Consejo Nacional de Ciencia y Tecnología).

Literature Cited

Ahn, S. H., W. L. Cheung, J. Y. Hsu, R. L. Diaz, M. M. Smith *et al.*, 2005 Sterile 20 kinase phosphorylates histone H2B at serine 10 during hydrogen peroxide-induced apoptosis in *S. cerevisiae*. Cell 120: 25–36.

Allis, C. D., S. L. Berger, J. Côté, S. Dent, T. Jenuwien *et al.*, 2007 New nomenclature for chromatin-modifying enzymes. Cell 131: 633–636.

Åström, S. U., S. M. Okamura, and J. Rine, 1999 Yeast cell-type regulation of DNA repair. Nature 397: 310.

Avvakumov, N., and J. Côté, 2007 The MYST family of histone acetyltransferases and their intimate links to cancer. Oncogene 26: 5395–5407.

Baker, L. A., B. M. Ueberheide, S. Dewell, B. T. Chait, D. Zheng *et al.*, 2013 The yeast Snt2 protein coordinates the transcriptional response to hydrogen peroxide-mediated oxidative stress. Mol. Cell. Biol. 33: 3735–3748.

Bedalov, A., M. Hirao, J. Posakony, M. Nelson, and J. A. Simon, 2003 NAD+-dependent deacetylase Hst1p controls biosynthesis and cellular NAD+ levels in *Saccharomyces cerevisiae*. Mol. Cell. Biol. 23: 7044–7054.

Bernstein, B. E., J. K. Tong, and S. L. Schreiber, 2000 Genomewide studies of histone deacetylase function in yeast. Proc. Natl. Acad. Sci. USA 97: 13708–13713.

Betermier, M., P. Bertrand, and B. S. Lopez, 2014 Is non-homologous end-joining really an inherently error-prone process? PLoS Genet. 10: e1004086.

Bird, A. W., D. Y. Yu, M. G. Pray-Grant, Q. Qiu, K. E. Harmon *et al.*, 2002 Acetylation of histone H4 by Esa1 is required for DNA double-strand break repair. Nature 419: 411–415.

Biswas, D., S. Takahata, and D. J. Stillman, 2008 Different genetic functions for the Rpd3(L) and Rpd3(S) complexes suggest competition between NuA4 and Rpd3(S). Mol. Cell. Biol. 28: 4445–4458.

Bond, J. F., J. L. Fridovich-Keil, L. Pillus, R. C. Mulligan, and F. Solomon, 1986 A chicken-yeast chimeric beta-tubulin protein is incorporated into mouse microtubules in vivo. Cell 44: 461–468.

Boudreault, A. A., D. Cronier, W. Selleck, N. Lacoste, R. T. Utley *et al.*, 2003 Yeast enhancer of polycomb defines global Esa1-dependent acetylation of chromatin. Genes Dev. 17: 1415–1428.

Brachmann, C. B., J. M. Sherman, S. E. Devine, E. E. Cameron, L. Pillus *et al.*, 1995 The *SIR2* gene family, conserved from bacteria to humans, functions in silencing, cell cycle progression, and chromosome stability. Genes Dev. 9: 2888–2902.

Campos, E. I., and D. Reinberg, 2009 Histones: annotating chromatin. Annu. Rev. Genet. 43: 559–599.

Carrozza, M. J., L. Florens, S. K. Swanson, W. J. Shia, S. Anderson *et al.*, 2005a Stable incorporation of sequence specific repressors

Ash1 and Ume6 into the Rpd3L complex. Biochim. Biophys. Acta 1731: 77–87.

Carrozza, M. J., B. Li, L. Florens, T. Suganuma, S. K. Swanson *et al.*, 2005b Histone H3 methylation by Set2 directs deacetylation of coding regions by Rpd3S to suppress spurious intragenic transcription. Cell 123: 581–592.

Chang, C. S., and L. Pillus, 2009 Collaboration between the essential Esa1 acetyltransferase and the Rpd3 deacetylase is mediated by H4K12 histone acetylation in *Saccharomyces cerevisiae*. Genetics 183: 149–160.

Chang, C. S., A. Clarke, and L. Pillus, 2012 Suppression analysis of *esa1* mutants in *Saccharomyces cerevisiae* links *NAB3* to transcriptional silencing and nucleolar functions. G3 2: 1223–1232.

Chapman, J. R., M. R. Taylor, and S. J. Boulton, 2012 Playing the end game: DNA double-strand break repair pathway choice. Mol. Cell 47: 497–510.

Chen, X. F., B. Kuryan, T. Kitada, N. Tran, J. Y. Li *et al.*, 2012 The Rpd3 core complex is a chromatin stabilization module. Curr. Biol. 22: 56–63.

Clarke, A. S., J. E. Lowell, S. J. Jacobson, and L. Pillus, 1999 Esa1p is an essential histone acetyltransferase required for cell cycle progression. Mol. Cell. Biol. 19: 2515–2526.

Clarke, A. S., E. Samal, and L. Pillus, 2006 Distinct roles for the essential MYST family HAT Esa1p in transcriptional silencing. Mol. Biol. Cell 17: 1744–1757.

Dang, W., K. K. Steffen, R. Perry, J. A. Dorsey, F. B. Johnson *et al.*, 2009 Histone H4 lysine 16 acetylation regulates cellular lifespan. Nature 459: 802–807.

Decker, P. V., D. Y. Yu, M. Iizuka, Q. Qiu, and M. M. Smith, 2008 Catalytic-site mutations in the MYST family histone acetyltransferase Esa1. Genetics 178: 1209–1220.

Dion, M. F., S. J. Altschuler, L. F. Wu, and O. J. Rando, 2005 Genomic characterization reveals a simple histone H4 acetylation code. Proc. Natl. Acad. Sci. USA 102: 5501–5506.

Dora, E. G., N. Rudin, J. R. Martell, M. S. Esposito, and R. M. Ramirez, 1999 *RPD3* (*REC3*) mutations affect mitotic recombination in *Saccharomyces cerevisiae*. Curr. Genet. 35: 68–76.

Drouin, S., L. Laramee, P. E. Jacques, A. Forest, M. Bergeron *et al.*, 2010 DSIF and RNA polymerase II CTD phosphorylation coordinate the recruitment of Rpd3S to actively transcribed genes. PLoS Genet. 6: e1001173.

Felsenfeld, G., and M. Groudine, 2003 Controlling the double helix. Nature 421: 448–453.

Feser, J., D. Truong, C. Das, J. J. Carson, J. Kieft *et al.*, 2010 Elevated histone expression promotes life span extension. Mol. Cell 39: 724–735.

Frye, R. A., 2000 Phylogenetic classification of prokaryotic and eukaryotic Sir2-like proteins. Biochem. Biophys. Res. Commun. 273: 793–798.

Gorrini, C., M. Squatrito, C. Luise, N. Syed, D. Perna *et al.*, 2007 Tip60 is a haplo-insufficient tumour suppressor required for an oncogene-induced DNA damage response. Nature 448: 1063–1067.

Gottlieb, S., and R. E. Esposito, 1989 A new role for a yeast transcriptional silencer gene, *SIR2*, in regulation of recombination in ribosomal DNA. Cell 56: 771–776.

Govind, C. K., H. Qiu, D. S. Ginsburg, C. Ruan, K. Hofmeyer *et al.*, 2010 Phosphorylated Pol II CTD recruits multiple HDACs, including Rpd3C(S), for methylation-dependent deacetylation of ORF nucleosomes. Mol. Cell 39: 234–246.

Haber, J. E., 2012 Mating-type genes and *MAT* switching in *Saccharomyces cerevisiae*. Genetics 191: 33–64.

Hampsey, M., 1997 A review of phenotypes in *Saccharomyces cerevisiae*. Yeast 13: 1099–1133.

Jazayeri, A., A. D. McAinsh, and S. P. Jackson, 2004 *Saccharomyces cerevisiae* Sin3p facilitates DNA double-strand break repair. Proc. Natl. Acad. Sci. USA 101: 1644–1649.

Kaluarachchi, D. S., H. Friesen, A. Baryshnikova, J. P. Lambert, Y. T. Chong *et al.*, 2012 Exploring the yeast acetylome using functional genomics. Cell 149: 936–948.

Keogh, M. C., S. K. Kurdistani, S. A. Morris, S. H. Ahn, V. Podolny *et al.*, 2005 Cotranscriptional Set2 methylation of histone H3 lysine 36 recruits a repressive Rpd3 complex. Cell 123: 593–605.

Kizer, K. O., T. Xiao, and B. D. Strahl, 2006 Accelerated nuclei preparation and methods for analysis of histone modifications in yeast. Methods 40: 296–302.

Kornberg, R. D., and Y. Lorch, 1999 Twenty-five years of the nucleosome, fundamental particle of the eukaryote chromosome. Cell 98: 285–294.

Krogan, N. J., J. Dover, S. Khorrami, J. F. Greenblatt, J. Schneider *et al.*, 2002 COMPASS, a histone H3 (lysine 4) methyltransferase required for telomeric silencing of gene expression. J. Biol. Chem. 277: 10753–10755.

Lafon, A., C. S. Chang, E. M. Scott, S. J. Jacobson, and L. Pillus, 2007 MYST opportunities for growth control: yeast genes illuminate human cancer gene functions. Oncogene 26: 5373–5384.

Lechner, T., M. J. Carrozza, Y. Yu, P. A. Grant, A. Eberharter *et al.*, 2000 Sds3 (suppressor of defective silencing 3) is an integral component of the yeast Sin3-Rpd3 histone deacetylase complex and is required for histone deacetylase activity. J. Biol. Chem. 275: 40961–40966.

Lee, S. E., F. Paques, J. Sylvan, and J. E. Haber, 1999 Role of yeast *SIR* genes and mating type in directing DNA double-strand breaks to homologous and non-homologous repair paths. Curr. Biol. 9: 767–770.

Lin, Y. Y., Y. Qi, J. Y. Lu, X. Pan, D. S. Yuan *et al.*, 2008 A comprehensive synthetic genetic interaction network governing yeast histone acetylation and deacetylation. Genes Dev. 22: 2062–2074.

Lin, Y. Y., J. Y. Lu, J. Zhang, W. Walter, W. Dang *et al.*, 2009 Protein acetylation microarray reveals that NuA4 controls key metabolic target regulating gluconeogenesis. Cell 136: 1073–1084.

Lu, J. Y., Y. Y. Lin, J. C. Sheu, J. T. Wu, F. J. Lee *et al.*, 2011 Acetylation of yeast AMPK controls intrinsic aging independently of caloric restriction. Cell 146: 969–979.

Maltby, V. E., and B. J. Martin, J. Brind'Amour, A. T. Chruscicki, K. L. McBurney *et al.*, 2012 Histone H3K4 demethylation is negatively regulated by histone H3 acetylation in *Saccharomyces cerevisiae*. Proc. Natl. Acad. Sci. USA 109: 18505–18510.

McCord, R. A., E. Michishita, T. Hong, E. Berber, L. D. Boxer *et al.*, 2009 SIRT6 stabilizes DNA-dependent protein kinase at chromatin for DNA double-strand break repair. Aging 1: 109–121.

McDaniel, S. L., and B. D. Strahl, 2013 Stress-free with Rpd3: a unique chromatin complex mediates the response to oxidative stress. Mol. Cell. Biol. 33: 3726–3727.

Merker, J. D., M. Dominska, P. W. Greenwell, E. Rinella, D. C. Bouck *et al.*, 2008 The histone methylase Set2p and the histone deacetylase Rpd3p repress meiotic recombination at the *HIS4* meiotic recombination hotspot in *Saccharomyces cerevisiae*. DNA Repair (Amst.) 7: 1298–1308.

Mieczkowski, P. A., M. Dominska, M. J. Buck, J. D. Lieb, and T. D. Petes, 2007 Loss of a histone deacetylase dramatically alters the genomic distribution of Spo11p-catalyzed DNA breaks in *Saccharomyces cerevisiae*. Proc. Natl. Acad. Sci. USA 104: 3955–3960.

Mitchell, L., J. P. Lambert, M. Gerdes, A. S. Al-Madhoun, I. S. Skerjanc *et al.*, 2008 Functional dissection of the NuA4 histone acetyltransferase reveals its role as a genetic hub and that Eaf1 is essential for complex integrity. Mol. Cell. Biol. 28: 2244–2256.

Mitchell, L., A. Lau, J. P. Lambert, H. Zhou, Y. Fong *et al.*, 2011 Regulation of septin dynamics by the *Saccharomyces cerevisiae* lysine acetyltransferase NuA4. PLoS ONE 6: e25336.

Mitchell, L., S. Huarda, M. Cotruta, R. Pourhanifeh-Lemeria, A. Steunoub *et al.*, 2013 mChIP-KAT-MS, a method to map protein interactions and acetylation sites for lysine acetyltransferases. Proc. Natl. Acad. Sci. USA 110: E1641–E1650.

Nakanishi, S., B. W. Sanderson, K. M. Delventhal, W. D. Bradford, K. Staehling-Hampton *et al.*, 2008 A comprehensive library of histone mutants identifies nucleosomal residues required for H3K4 methylation. Nat. Struct. Mol. Biol. 15: 881–888.

Natsume-Kitatani, Y., M. Shiga, and H. Mamitsuka, 2011 Genome-wide integration on transcription factors, histone acetylation and gene expression reveals genes co-regulated by histone modification patterns. PLoS ONE 6: e22281.

Nitiss, J., and J. C. Wang, 1988 DNA topoisomerase-targeting antitumor drugs can be studied in yeast. Proc. Natl. Acad. Sci. USA 85: 7501–7505.

Pijnappel, W. W., D. Schaft, A. Roguev, A. Shevchenko, H. Tekotte *et al.*, 2001 The *S. cerevisiae* SET3 complex includes two histone deacetylases, Hos2 and Hst1, and is a meiotic-specific repressor of the sporulation gene program. Genes Dev. 15: 2991–3004.

Prelich, G., 1999 Suppression mechanisms: themes from variations. Trends Genet. 15: 261–266.

Rando, O. J., and F. Winston, 2012 Chromatin and transcription in yeast. Genetics 190: 351–387.

Reid, J. L., V. R. Iyer, P. O. Brown, and K. Struhl, 2000 Coordinate regulation of yeast ribosomal protein genes is associated with targeted recruitment of Esa1 histone acetylase. Mol. Cell 6: 1297–1307.

Robyr, D., Y. Suka, I. Xenarios, S. K. Kurdistani, A. Wang *et al.*, 2002 Microarray deacetylation maps determine genome-wide functions for yeast histone deacetylases. Cell 109: 437–446.

Roy, N., and K. W. Runge, 2000 Two paralogs involved in transcriptional silencing that antagonistically control yeast lifespan. Curr. Biol. 10: 111–114.

Ruiz-Roig, C., C. Vieitez, and F. Posas, and E. de Nadal, 2010 The Rpd3L HDAC complex is essential for the heat stress response in yeast. Mol. Microbiol. 76: 1049–1062.

Sardiu, M. E., J. M. Gilmore, M. J. Carrozza, B. Li, J. L. Workman *et al.*, 2009 Determining protein complex connectivity using a probabilistic deletion network derived from quantitative proteomics. PLoS ONE 4: e7310.

Scott, E. M., and L. Pillus, 2010 Homocitrate synthase connects amino acid metabolism to chromatin functions through Esa1 and DNA damage. Genes Dev. 24: 1903–1913.

Shahbazian, M. D., and M. Grunstein, 2007 Functions of site-specific histone acetylation and deacetylation. Annu. Rev. Biochem. 76: 75–100.

Shevchenko, A., and A. Roguev, D. Schaft, L. Buchanan, B. Habermann *et al.*, 2008 Chromatin Central: towards the comparative proteome by accurate mapping of the yeast proteomic environment. Genome Biol. 9: RI67.

Smith, E. R., A. Eisen, W. Gu, M. Sattah, A. Pannuti *et al.*, 1998 *ESA1* is a histone acetyltransferase that is essential for growth in yeast. Proc. Natl. Acad. Sci. USA 95: 3561–3565.

Smith, J. S., C. B. Brachmann, I. Celic, M. A. Kenna, S. Muhammad *et al.*, 2000 A phylogenetically conserved NAD+-dependent protein deacetylase activity in the Sir2 protein family. Proc. Natl. Acad. Sci. USA 97: 6658–6663.

Squatrito, M., C. Gorrini, and B. Amati, 2006 Tip60 in DNA damage response and growth control: many tricks in one HAT. Trends Cell Biol. 16: 433–442.

Su, Y., A. B. Barton, and D. B. Kaback, 2000 Decreased meiotic reciprocal recombination in subtelomeric regions in *Saccharomyces cerevisiae*. Chromosoma 109: 467–475.

Tamburini, B. A., and J. K. Tyler, 2005 Localized histone acetylation and deacetylation triggered by the homologous recombination pathway of double-strand DNA repair. Mol. Cell. Biol. 25: 4903–4913.

Turner, E. L., M. E. Malo, M. G. Pisclevich, M. D. Dash, G. F. Davies *et al.*, 2010 The *Saccharomyces cerevisiae* anaphase-promoting complex interacts with multiple histone-modifying enzymes to regulate cell cycle progression. Eukaryot. Cell 9: 1418–1431.

Valencia, M., M. Bentele, M. B. Vaze, G. Herrmann, E. Kraus *et al.*, 2001 *NEJ1* controls non-homologous end joining in *Saccharomyces cerevisiae*. Nature 414: 666–669.

Vogelauer, M., J. Wu, N. Suka, and M. Grunstein, 2000 Global histone acetylation and deacetylation in yeast. Nature 408: 495–498.

Xu, Y., and B. D. Price, 2011 Chromatin dynamics and the repair of DNA double strand breaks. Cell Cycle 10: 261–267.

Yan, Y., S. Harper, D. W. Speicher, and R. Marmorstein, 2002 The catalytic mechanism of the *ESA1* histone acetyltransferase involves a self-acetylated intermediate. Nat. Struct. Biol. 9: 862–869.

Yang, X. J., and E. Seto, 2008 The Rpd3/Hda1 family of lysine deacetylases: from bacteria and yeast to mice and men. Nat. Rev. Mol. Cell Biol. 9: 206–218.

Yi, C., M. Ma, L. Ran, J. Zheng, J. Tong *et al.*, 2012 Function and molecular mechanism of acetylation in autophagy regulation. Science 336: 474–477.

Zhang, L., N. Liu, X. Ma, and L. Jiang, 2013 The transcriptional control machinery as well as the cell wall integrity and its regulation are involved in the detoxification of the organic solvent dimethyl sulfoxide in *Saccharomyces cerevisiae*. FEMS Yeast Res. 13: 200–218.

Zhang, W., J. R. Bone, D. G. Edmondson, B. M. Turner, and S. Y. Roth, 1998 Essential and redundant functions of histone acetylation revealed by mutation of target lysines and loss of the Gcn5p acetyltransferase. EMBO J. 17: 3155–3167.

Zhou, J., B. O. Zhou, B. A. Lenzmeier, and J. Q. Zhou, 2009 Histone deacetylase Rpd3 antagonizes Sir2-dependent silent chromatin propagation. Nucleic Acids Res. 37: 3699–3713.

Communicating editor: M. Hampsey

GENETICS

Supporting Information
http://www.genetics.org/lookup/suppl/doi:10.1534/genetics.114.165894/-/DC1

Bypassing the Requirement for an Essential MYST Acetyltransferase

Ana Lilia Torres-Machorro and Lorraine Pillus

DOI: 10.1534/genetics.114.165894

Table S1 Yeast strains

Strain	Genotype	Reference
LPY5 (W303-1a)	MAT*α ade2-1 can1-100 his3-11,15 leu2-3,112 trp1-1 ura3-1*	R. Rothstein
LPY79	*W303* MAT*α*	
YCB232 (LPY1081)	MAT*α ade2-101 his3Δ200 leu2Δ1 lys2-801 trp1Δ63 ura3-52 hst1Δ2::LEU2*	
LPY4767	*W303* MAT*α rDNA::ADE2-CAN1*	
LPY4776	*W303* MAT*α esa1-414*	
LPY4911	*W303* MAT*α esa1-414 rDNA::ADE2-CAN1*	Clarke et al. 2006
LPY10700	*LPY12232 + pLP1971 (no pJH33)*	
LPY12205	*W303* MAT*α esa1Δ::HIS3 + pLP796*	
LPY12207	*W303* MAT*α esa1Δ::HIS3 rpd3Δ::kanMX + pLP796*	
LPY12232	*W303* MAT*α hht1-hhf1Δ::kanMX hht2-hhf2Δ::kanMX hta2-htb2Δ::HPH + pJH33*	Chang and Pillus 2009
LPY12885	*W303* MAT*α hda1Δ::TRP1*	
LPY12959	*W303* MAT*α sds3Δ::kanMX*	
LPY13059	*LPY12232 + pLP1990 (no pJH33)*	Chang and Pillus 2009
LPY13060	*LPY12232 + pLP2146 (no pJH33)*	Chang and Pillus 2009
LPY13061	*LPY12232 + pLP2181 (no pJH33)*	Chang and Pillus 2009
LPY14161	*LPY12232 + pLP1775 (no pJH33)*	Chang and Pillus 2009
LPY14162	*LPY12232 + pLP2145 (no pJH33)*	Chang and Pillus 2009
LPY15908	*LPY12232 + pLP1777 (no pJH33)*	
LPY16480	*W303* MAT*α esa1Δ::HIS3 sds3Δ::kanMX + pLP796*	
LPY16595	*W303* MAT*α esa1Δ::HIS3 sds3Δ::kanMX*	
LPY17027	*W303* MAT*α esa1Δ::HIS3 pho23Δ::kanMX + pLP796*	
LPY17029	*W303* MAT*α esa1Δ::HIS3 rco1::kanMX + pLP796*	
LPY17145	*W303* MAT*α esa1Δ::HIS3 sds3Δ::kanMX hht1-hhf1Δ::kanMX hht2-hhf2Δ::kanMX hta2-htb2Δ::HPH + pJH33*	
LPY17271	*LPY17145 + pLP2145 (no pJH33)*	
LPY17272	*LPY17145 + pLP2181 (no pJH33)*	
LPY17273	*LPY17145 + pLP2146 (no pJH33)*	
LPY17274	*LPY17145 + pLP2183 (no pJH33)*	
LPY17368	*LPY17145 + pLP1775 (no pJH33)*	
LPY17369	*LPY17145 + pLP1990 (no pJH33)*	
LPY17713	*W303* MAT*α esa1Δ::HIS3 rpd3Δ::LEU2 + pLP796*	
LPY17714	*W303* MAT*α esa1Δ::HIS3 sds3Δ::kanMX rpd3Δ::LEU2 + pLP796*	
LPY17724	*W303* MAT*α sds3Δ::kanMX hos2Δ::TRP1*	
LPY17748	*W303* MAT*α esa1Δ::HIS3 sds3Δ::kanMX hda1Δ::TRP1*	
LPY17753	*W303* MAT*α sds3Δ::kanMX hda1Δ::TRP1*	
LPY17759	*W303* MAT*α esa1Δ::HIS3 sds3Δ::kanMX hda1Δ::TRP1 + pLP796*	
LPY17761	*W303* MAT*α esa1Δ::HIS3 hda1Δ::TRP1 + pLP796*	
LPY17799	*W303* MAT*α esa1Δ::HIS3 hst1Δ2::LEU2 + pLP796*	
LPY17801	*W303* MAT*α esa1Δ::HIS3 sds3Δ::kanMX hst1Δ2::LEU2 + pLP796*	
LPY17805	*W303* MAT*α esa1Δ::HIS3 sds3Δ::kanMX rco1Δ::kanMX + pLP796*	
LPY17845	*W303* MAT*α esa1Δ::HIS3 hos2Δ::TRP1 + pLP796*	
LPY17848	*W303* MAT*α esa1Δ::HIS3 sds3Δ::kanMX hos2Δ::TRP1 + pLP796*	
LPY17900	*W303* MAT*α esa1Δ::HIS3 sds3Δ::kanMX hst1Δ2::LEU2*	
LPY17959	*W303* MAT*α esa1Δ::HIS3 sds3Δ::kanMX rDNA::ADE2-CAN1*	

LPY17966	*W303* MAT*α esa1Δ::HIS3 sds3Δ::kanMX sir2Δ::TRP1 + pLP796*
LPY17968	*W303* MAT*α esa1Δ::HIS3 sir2Δ::TRP1 + pLP796*
LPY17969	*W303* MAT*α sds3Δ::kanMX sir2Δ::TRP1*
LPY17997	*W303* MAT*α esa1Δ::HIS3 sds3Δ::kanMX sir2Δ::TRP1*
LPY18032	*W303* MAT*α esa1Δ::HIS3 sin3Δ::kanMX + pLP796*
LPY18095	*W303* MAT*α hst1Δ2::LEU2*
LPY18096	*W303* MAT*α hst1Δ2::LEU2*
LPY18112	*W303* MAT*α sds3Δ::kanMX hst1Δ2::LEU2*
LPY18210	*W303* MAT*α esa1Δ::HIS3 sds3Δ::kanMX hst1Δ2::LEU2 rDNA::ADE2-CAN1*
LPY18222	*W303* MAT*α esa1Δ::HIS3 sds3Δ::kanMX hda1Δ::TRP1 rDNA::ADE2-CAN1*
LPY18223	*W303* MAT*α sir2Δ::kanMX*
LPY18226	*W303* MAT*α sds3Δ::kanMX rco1Δ::kanMX*
LPY18573	*W303* MAT*α esa1Δ::HIS3 sds3Δ::kanMX sir2Δ::TRP1 rDNA::ADE2-CAN1*
LPY18595	*W303* MAT*α sds3Δ::kanMX rpd3Δ::LEU2*
LPY19307	*LPY12232 + pLP2208 (no pJH33)*
LPY19437	*LPY12232 + pLP2183 (no pJH33)*
LPY20385	*W303* MAT*α esa1Δ::HIS3 dep1Δ::HIS3 + pLP796*
LPY20387	*LPY17145 + pLP1787 (no pJH33)*
LPY20388	*LPY17145 + pLP3022 (no pJH33)*
LPY20389	*LPY17145 + pLP3018 (no pJH33)*
LPY20431	*LPY17145 + pLP2138 (no pJH33)*
LPY20430	*LPY17145 + pLP2185 (no pJH33)*
LPY20432	*LPY17145 + pLP2142 (no pJH33)*
LPY20434	*LPY17145 + pLP2208 (no pJH33)*
LPY20435	*LPY17145 + pLP2244 (no pJH33)*
LPY20436	*LPY17145 + pLP1971 (no pJH33)*
LPY20437	*LPY17145 + pLP1777 (no pJH33)*
LPY20465	*W303* MAT*α esa1Δ::HIS3 sap30Δ::kanMX + pLP796*
LPY20625	*LPY12232 + pLP2185 (no pJH33)*
LPY20626	*LPY12232 + pLP2138 (no pJH33)*
LPY20627	*LPY12232 + pLP2142 (no pJH33)*
LPY20628	*LPY12232 + pLP2242 (no pJH33)*
LPY20629	*LPY12232 + pLP3018 (no pJH33)*
LPY20630	*LPY12232 + pLP1787 (no pJH33)*
LPY20631	*LPY12232 + pLP3022 (no pJH33)*
LPY20632	*LPY12232 + pLP3233 (no pJH33)*
LPY20633	*LPY12232 + pLP2244 (no pJH33)*
LPY20661	*LPY17145 + pLP3233 (no pJH33)*
LPY20662	*LPY17145 + pLP2242 (no pJH33)*
LPY20664	*W303* MAT*α esa1Δ::HIS3 snt2Δ::kanMX + pLP796*

Unless referenced, strains were constructed in this study.

Table S2 Plasmids

Plasmid	Description	Source/Reference
pJH33	*HTA1 HTB1 HHF2 HHT2 URA3 CEN*	Ahn et al. 2005
pLP126	*pRS316 URA3 CEN*	
pLP136	*URA3 2μ*	
pLP287	*SAS2 URA3 2μ*	
pLP641	*SAS3 URA3 2μ*	
pLP796	*ESA1 URA3 2μ*	Clarke et al. 2006
pLP940	*HAT1 URA3 2μ*	
pLP1641	*GCN5 URA3 2μ*	
pLP1775	*HHF2 HHT2 TRP1 CEN*	S. L. Berger
pLp1777	*HHF2 hht2-K14A TRP1 CEN*	
pLP1787	*HHF2 hht2-K9A TRP1 CEN*	
pLP1971	*hhf2-K5Q,K8Q,K12Q HHT2 TRP1 CEN*	
pLP1990	*hhf2-K16A HHT2 TRP1 CEN*	Chang and Pillus , 2009
pLP2138	*hhf2-K8R HHT2 TRP1 CEN*	
pLP2142	*hhf2-K12R HHT2 TRP1 CEN*	
pLP2145	*hhf2-K8A HHT2 TRP1 CEN*	Chang and Pillus 2009
pLP2146	*hhf2-K12A HHT2 TRP1 CEN*	Chang and Pillus 2009
pLP2181	*hhf2-K5A HHT2 TRP1 CEN*	Chang and Pillus 2009
pLP2183	*hhf2-K5Q HHT2 TRP1 CEN*	
pLP2185	*hhf2-K5R HHT2 TRP1 CEN*	
pLP2208	*hhf2-K8A,K12A HHT2 TRP1 CEN*	
pLP2242	*hhf2-K16R HHT2 TRP1 CEN*	
pLP2244	*hhf2-K8Q,K12Q HHT2 TRP1 CEN*	
pLP3018	*HHF2 hht2-K14R TRP1 CEN*	
pLP3022	*HHF2 hht2-K9R TRP1 CEN*	
pLP3233	*HHF2 hht2-K9Q TRP1 CEN*	

Table S3 Oligonucleotides

Oligo	Name	Sequence
oLP858	H4K5Q-F	TCCGGTAGAGGTCAAGGTGGTAAAGG
oLP859	H4K5Q-R	CCTTTACCACCTTGACCTCTACCGGA
oLP1669	HST1-KO-F	GCAATTCTGGTAGCAATGAC
oLP1670	HST1-KO-R	GAGGTGCAAGAGTCTAATC
oLP2054	H3K9Q-F	CTAAACAAACAGCTAGACAATCCACTGGTGG
oLP2055	H3K9Q-R	CCACCAGTGGATTGTCTAGCTGTTTGTTTAG
oLP2078	SNT2-KO-F	CAGGCTGGGAACCAGGGAATG
oLP2079	SNT2-KO-R	GCCAGGCGCGAGGATTTTAGC

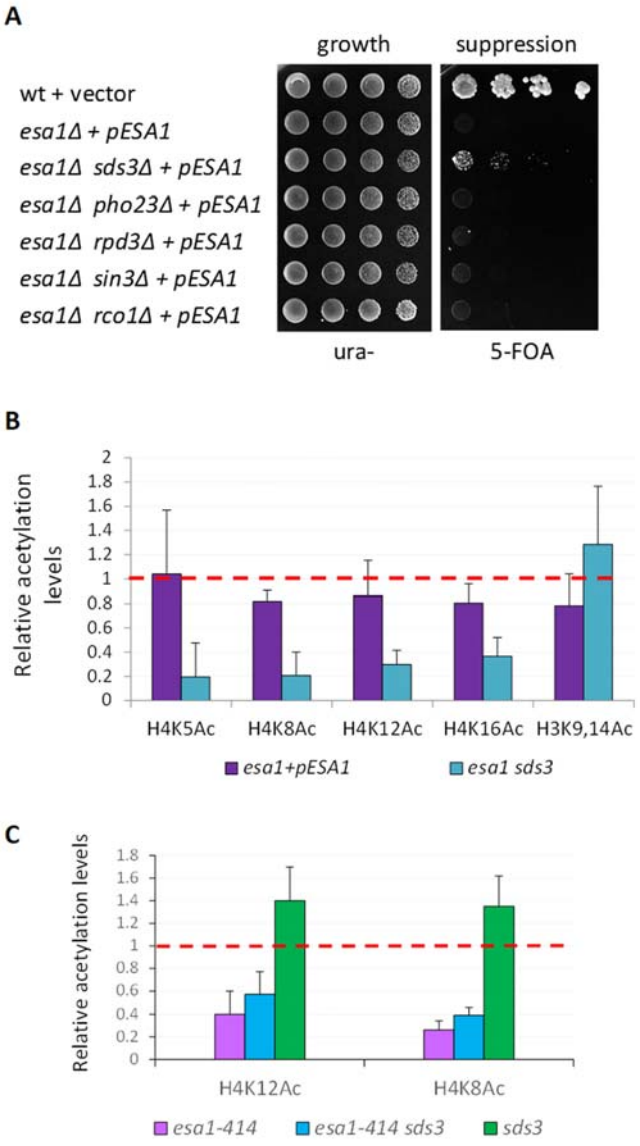

Figure S1 Further characterization of successful and failed bypass suppressors.
(A) Growth of *esa1Δ sds3Δ* was slow compared to wild-type. Assay as in Figure 1B, but including the wild-type strain (LPY79) transformed with a *URA3* vector. Depletion of nutrients in the medium due to the rapid growth of the wild-type strain prevented more extensive growth of *esa1Δ sds3Δ*. If the plating of the bypass strain was closer to rapid growing strains, its growth inhibition was more severe. (B) Histone H4 acetylation was low in *esa1Δ sds3Δ* cells, whereas H3 acetylation was comparable to wild-type levels. Histone H4 acetylation levels at specified lysines were quantified from two or more independent immunoblots and normalized relative to histone H4 levels. Histone H3K9, K14Ac levels were normalized to histone H3. Values were graphed relative to wild-type (red dashed line) for *esa1Δ +pESA1* and *esa1Δ sds3Δ* strains. The H4 acetylation levels at all lysines tested in *esa1Δ sds3Δ* were statistically lower than wild-type $p<0.0001$, whereas H3 acetylation remained similar to wild-type. (C) Deletion of *SDS3* suppressed low H4 acetylation in *esa1-414* cells grown at 37°. Quantification of two independent immunoblots including those shown in Figure 1G. Graphs and normalization were as in Figure S1B.

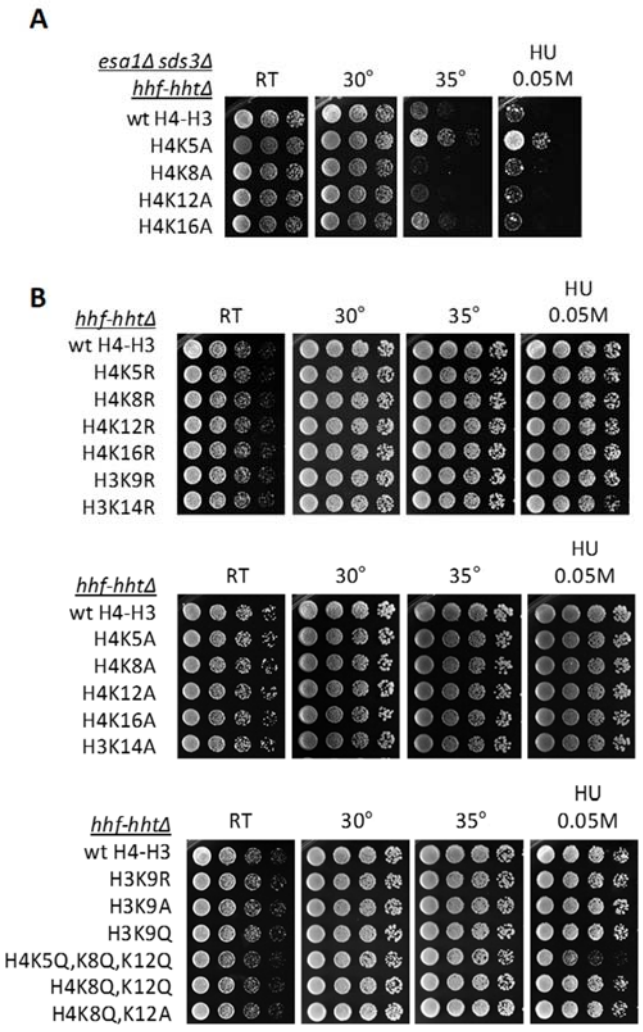

Figure S2 Histone mutants controls.
(A) Phenotypes of histone H4 lysine to alanine mutations in the *esa1Δ sds3Δ hht1-hhf1Δ hht2-hhf2Δ* background. Tested strains included the following histone mutations: wild-type histones H3-H4 (LPY17368), H4K5A (LPY17272), H4K8A (LPY17271), H4K12A (LPY17273) and H4K16A (LPY17369). (B) Histone mutants in the wild-type background are not independently sensitive to environmental challenges. Strains were deleted for genes encoding all copies of H3 and H4 *(hht-hhfΔ)* and carried a plasmid with either wild type H3 and H4 or with one mutated lysine in H4 or H3 as indicated. Wild type histones H3-H4 (LPY14161), H4K5R (LPY20625), H4K8R (LPY20626), H4K12R (LPY20627), H4K16R (LPY20628), H3K9R (LPY20631), H3K14R (LPY20629), H4K5A (LPY13061), H4K8A (LPY14162), H4K12A (LPY13060), H4K16A (LPY13059), H3K14A (LPY15908), H3K9A (LPY20630), H3K9Q (LPY20632), H4K5Q,K8Q,K12Q (LPY10700), H4K8,K12Q (LPY20633) and H4K8,12A (LPY19307) in the *hht1-hhf1Δ hht2-hhf2Δ* background were tested in serial dilutions on YPAD at room temperature, 30° and 35°. Hydroxyurea plates were grown at 30°. The combined H4K5Q,K8Q,K12Q mutant was previously found to be sensitive to DNA damage (Bird et al. 2002). The same mutant in the *esa1Δ sds3Δ* background suppressed temperature sensitivity, but not DNA damage sensitivity as expected (Figure 2E).

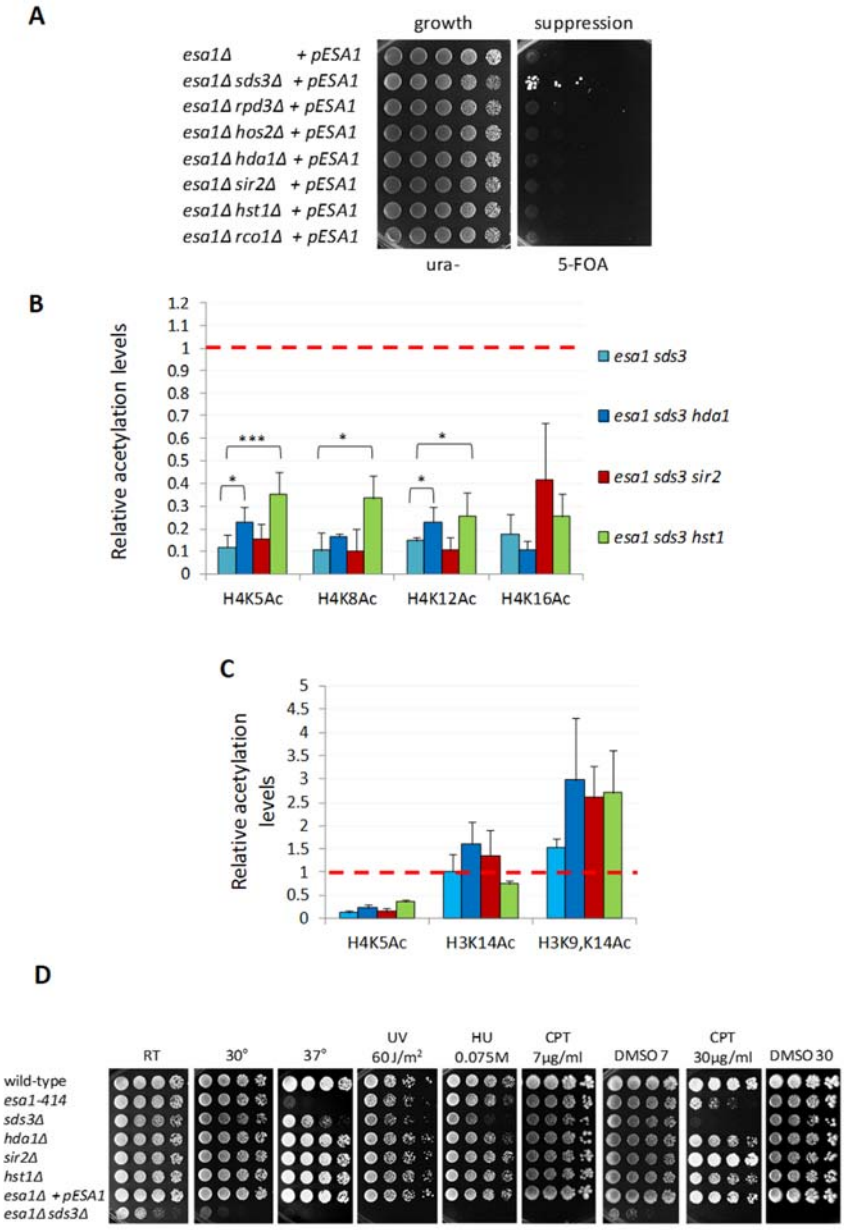

Figure S3 Double and single mutants with *SDS3* intact and histone acetylation ratio in *esa1Δ sds3Δ* HDAC-deleted strains.
(A) When *SDS3* was present, HDAC loss did not bypass *esa1Δ* lethality. *ESA1* covered strains *esa1Δ* (LPY12205), *esa1Δ sds3Δ* (LPY16480), *esa1Δ rpd3Δ* (LPY17713), *esa1Δ hda1Δ* (LPY17761), *esa1Δ hst1Δ* (LPY17799), *esa1Δ hos2Δ* (LPY17845), *esa1Δ sir2Δ* (LPY17968) and *esa1Δ rco1Δ* (LPY17029) were tested as in Fig. 3A. (B) High histone H3 / low histone H4 acetylation ratios were observed in *esa1Δ* bypass strains. Quantification of specific histone modifications in at least two independent blots, including blots in Figure 3B. The values were normalized as in Figure S1B. Histone H4K5, K8 and K12 acetylation levels were higher in the *esa1Δ sds3Δ hda1Δ* and *esa1Δ sds3Δ hst1Δ* strains relative to *esa1Δ sds3Δ. SIR2* and *HST1* deletions in *esa1Δ sds3Δ* strains suppressed low levels of histone H4K16 acetylation. Statistical significant differences were analyzed with the student's t test and are marked with * ($p<0.05$) and *** ($p<0.0001$). (C) Histone H3K14 and H3K9, K14 acetylation levels remain high in bypass suppressor strains. Values were quantified as in Figure S1B from at least two independent experiments and graphed relative to wild-type (red dashed line). Even though histone H3 acetylation is higher in *esa1Δ sds3Δ* HDAC-deleted strains, it was not significantly different from *esa1Δ sds3Δ* strains. (D) Phenotypes of single mutant strains. The *esa1-414* and *sds3Δ* strains were temperature- and DNA damage sensitive at high concentrations of CPT. Strains tested were: wild-type (LPY79), *esa1-414* (LPY4776), *sds3Δ* (LPY12959), *hda1Δ* (LPY12885), *sir2Δ* (LPY18223), *hst1Δ* (LPY18096), *esa1Δ+ pESA1* (LPY12205) and *esa1Δ sds3Δ* (LPY16595).